ChemPubSoc Europe

DOI: 10.1002/chem.201602074

CHEMISTRY A European Journal Full Paper

Coordination Chemistry

Surprisingly Different Reaction Behavior of Alkali and Alkaline Earth Metal Bis(trimethylsilyl)amides toward Bulky *N*-(2-Pyridylethyl)-*N*′-(2,6-diisopropylphenyl)pivalamidine

Diana Kalden, Ansgar Oberheide, Claas Loh, Helmar Görls, Sven Krieck, and Matthias Westerhausen*[a]

Dedicated to Professor Wolfgang Seidel on the occasion of his 85th birthday

Abstract: *N*-(2,6-Diisopropylphenyl)-*N*′-(2-pyridylethyl)pivalamidine (Dipp-N=C(*t*Bu)-N(H)-C_2H_4-Py) (**1**), reacts with metalation reagents of lithium, magnesium, calcium, and strontium to give the corresponding pivalamidinates [(tmeda)Li{Dipp-N=C(*t*Bu)-N-C_2H_4-Py}] (**6**), [Mg{Dipp-N=C(*t*Bu)-N-C_2H_4-Py}$_2$] (**3**), and heteroleptic [{$(Me_3Si)_2N$}Ae{Dipp-N=C(*t*Bu)-N-C_2H_4-Py}], with Ae being Ca (**2a**) and Sr (**2b**). In contrast to this straightforward deprotonation of the amidine units, the reaction of **1** with the bis(trimethylsilyl)amides of sodium or potassium unexpectedly leads to a β-metalation and an immediate deamidation reaction yielding [$(thf)_2$Na{Dipp-N=C(*t*Bu)-N(H)}] (**4a**) or [$(thf)_2$K{Dipp-N=C(*t*Bu)-N(H)}] (**4b**), respectively, as well as 2-vinylpyridine in both cases. The lithium derivative shows a similar reaction behavior to the alkaline earth metal congeners, underlining the diagonal relationship in the periodic table. Protonation of **4a** or the metathesis reaction of **4b** with CaI_2 in tetrahydrofuran yields *N*-(2,6-diisopropylphenyl)pivalamidine (Dipp-N=C(*t*Bu)-NH_2) (**5**), or [$(thf)_4$Ca{Dipp-N=C(*t*Bu)-N(H)}$_2$] (**7**), respectively. The reaction of $AN(SiMe_3)_2$ (A = Na, K) with less bulky formamidine Dipp-N=C(H)-N(H)-C_2H_4-Py (**8**) leads to deprotonation of the amidine functionality, and [(thf)Na{Dipp-N=C(H)-N-C_2H_4-Py}]$_2$ (**9a**) or [(thf)K{Dipp-N=C(H)-N-C_2H_4-Py}]$_2$ (**9b**), respectively, are isolated as dinuclear complexes. From these experiments it is obvious, that β-metalation/deamidation of *N*-(2-pyridylethyl)amidines requires bases with soft metal ions and also steric pressure. The isomeric forms of all compounds are verified by single-crystal X-ray structure analysis and are maintained in solution.

Introduction

Multidentate nitrogen donors represent widely used Lewis bases because they commonly form very stable complexes with electropositive (s-block) metals and transition metals.[1] Therefore, these ligands can often facially shield a metal ion and direct the attack of substrate molecules. Bulky β-diketiminates,[2] triazenides,[3] di- and tri(pyrazolyl)methanes and -methanides,[4] amidinates, and related anions such as guanidinates[5] represent prominent bi- and tridentate ligands that form very stable complexes with s-block metal ions. Spectacular examples include magnesium(I) complexes with Mg–Mg bonds of surprisingly high stability,[6] and an arylcalcium derivative with a pentafluorophenyl moiety.[7] The coordination behavior of amidinate and guanidinate anions with metal ions shows significant diversity due to the fact that both *anti/syn* and *E/Z*-isomerism are possible leading to four major alignments (Scheme 1). The coordination chemistry of these ligands is determined by whether the metal ions prefer π-interactions with aryl groups or the coordination of hard Lewis bases such as ethers. Lewis basic donor sites in the *N*-bound sidearm also strongly influence the coordination mode of this ligand.

The *N,N*′-bis(2,6-diisopropylphenyl)benz-[8,9] and -pivalamidinates[9,10] (R = Ph and *t*Bu, respectively) of potassium (Scheme 2, **A**) and calcium (Scheme 2, $\mathbf{B_1}$ and $\mathbf{B_2}$) bind through the nitrogen atoms and the negative charge is widely delocalized throughout the *syn-E*-isomeric 1,3-diazaallyl moiety in each case (the prefix *syn* or *anti* refer to the N-bound organic groups neglecting the metal atoms). The ytterbium (not shown) and samarium complexes (**C**) bind to the *anti-Z*-isomeric *N,N*′-bis(2,6-diisopropylphenyl)pivalamidinate resulting in strong metal π-interactions to one 2,6-diisopropylphenyl group (Dipp).[10] In contrast to this binding mode, the lanthanoids ytterbium, europium, and samarium bind only to the N atoms of the diazaallyl system of bulky *syn-E*-isomeric *N,N*′-bis(2,6-diisopropylphenyl)guanidinate ($\mathbf{B_2}$).[11] Substitution of one N-bound Dipp group by another substituent with a Lewis basic donor site offers the opportunity to locate the metal ion on a predetermined definite position with respect to the allyl system. Thus *anti-Z*-isomeric *N*-(2-pyridylmethyl)-[12] (**D**) and *N*-

[a] *D. Kalden, A. Oberheide, Dr. C. Loh, Dr. H. Görls, Dr. S. Krieck, Prof. Dr. M. Westerhausen*
Institute of Inorganic and Analytical Chemistry, Friedrich Schiller University Humboldstrasse 8, 07743 Jena (Germany)
http://www.lsac1.uni-jena.de
E-mail: m.we@uni-jena.de

Supporting information for this article is available on the WWW under http://dx.doi.org/10.1002/chem.201602074.

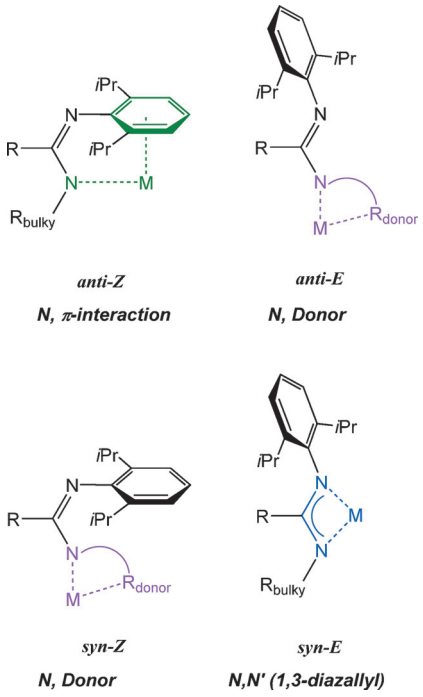

Scheme 1. General coordination modes of *N*-(2,6-diisopropylphenyl)amidinates (R = H, alkyl, aryl) and guanidinates (R = amino) in metal complexes. *Anti*-isomers are shown in the top row, *syn*-isomers in the bottom; *Z*-isomerism is depicted in the left column, *E*-isomerism in the right column. The colors signify different coordination modes.

(8-quinolyl)-*N*′-2,6-diisopropylphenylamidinate[13] (**E**) enforce calcium π-interactions with the 2,6-diisopropylphenyl group, whereas *anti*-*E*-isomeric *N*-(2-pyridyl)-*N*′-2,6-diisopropylphenylamidinate[13] (**F**) binds to calcium exclusively through the nitrogen bases. A longer alkyl bridge between the 1,3-diazaallyl system and the 2-pyridyl moiety leads to the *N*-(2-pyridylethyl)-*N*′-2,6-diisopropylphenylamidinate ion. A comparable binding motif to **E** and **F** was observed for the co-ligand-free magnesium complex with a hexa-coordinate alkaline earth metal atom bound to two *N*-(2-pyridylethyl)-*N*′-(3,5-dimethylphenyl)-4-methylbenzamidinate anions (not shown); all nitrogen bases were bound to the metal center leading to a distorted octahedral environment.[14]

Based on our earlier observation that a third Lewis base in a side arm of the amidinate ligand is able to stabilize calcium π-interactions with aryl groups,[12,13] we investigated compounds with an even longer alkyl spacer between the amidinate and the 2-pyridyl moieties.

Results and Discussion

Synthesis

The bulky tridentate Lewis base *N*-(2-pyridylethyl)-*N*′-(2,6-diisopropylphenyl)pivalamidine (**1**) was prepared by the reaction of *N*-(2,6-diisopropylphenyl)pivalimidoyl chloride[9,12,15] with an equimolar amount of 2-(aminoethyl)pyridine in boiling toluene (reaction 1). Recrystallization from toluene yielded the *syn*-*Z*-isomer of **1** in the crystalline state.

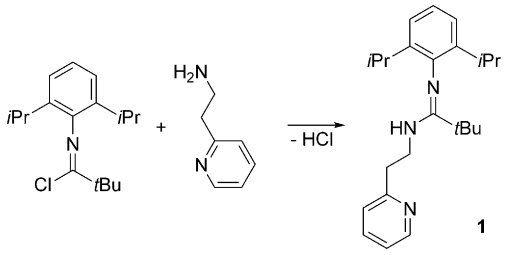

Generally, two established pathways allow for the synthesis of calcium complexes, namely (i) the metalation of the amidines with, for example, $[(thf)_2Ca\{N(SiMe_3)_2\}_2]$, and (ii) the metathetical approach of potassium amidinate with $[(thf)_4CaI_2]$ utilizing the insolubility of KI in ethereal solvents. Therefore, initial studies investigated the synthesis of the calcium derivative of the amidine **1** through the straightforward metalation route. The metalation reaction of *N*-(2-pyridylethyl)-*N*′-(2,6-diisopropylphenyl)pivalamidine (**1**) with $[(thf)_2Ae\{N(SiMe_3)_2\}_2]$ (Ae = Ca, Sr) in tetrahydrofuran (THF) yielded the ether-free heteroleptic complexes $[(Me_3Si)_2NAe\{tBuC(=NDipp)(-NCH_2CH_2Py)\}]$ [Ae = Ca (**2a**), Sr (**2b**)] according to reaction 2.

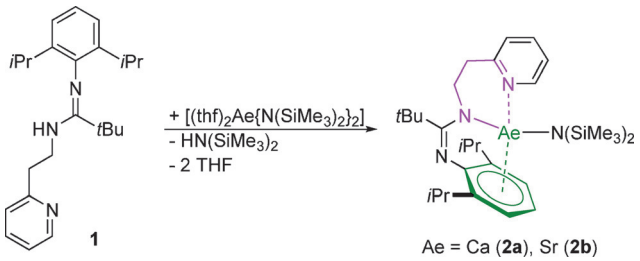

The harder magnesium ion prefers hard Lewis bases and metal π-interactions are disadvantageous in comparison to Mg–N bonds. To also study the coordination behavior of pivalamidine **1** toward Mg^{2+} ions, this amidine was metalated with dibutylmagnesium in aliphatic hydrocarbons (reaction 3).

To elucidate the alternative metathetical route, *N*-(2-pyridylethyl)-*N*′-(2,6-diisopropylphenyl)pivalamidine (**1**) was reacted

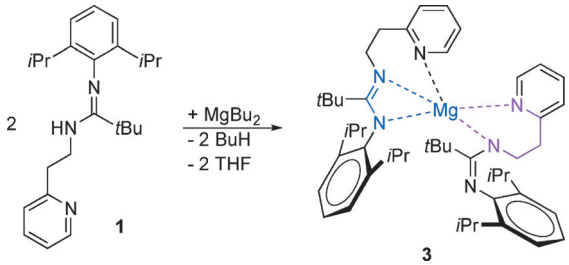

with KH in THF or $AN(SiMe_3)_2$ (A = Na, K) in toluene. In either case the cleavage of a C–N bond occurred with the loss of 2-vinylpyridine, which was identified by gas chromatography and NMR spectroscopy. Furthermore, the alkali metal-mediated cleavage of the C–N bond was also supported by a hydrolysis experiment that yielded Dipp-N=C(*t*Bu)-NH_2. Finally, the com-

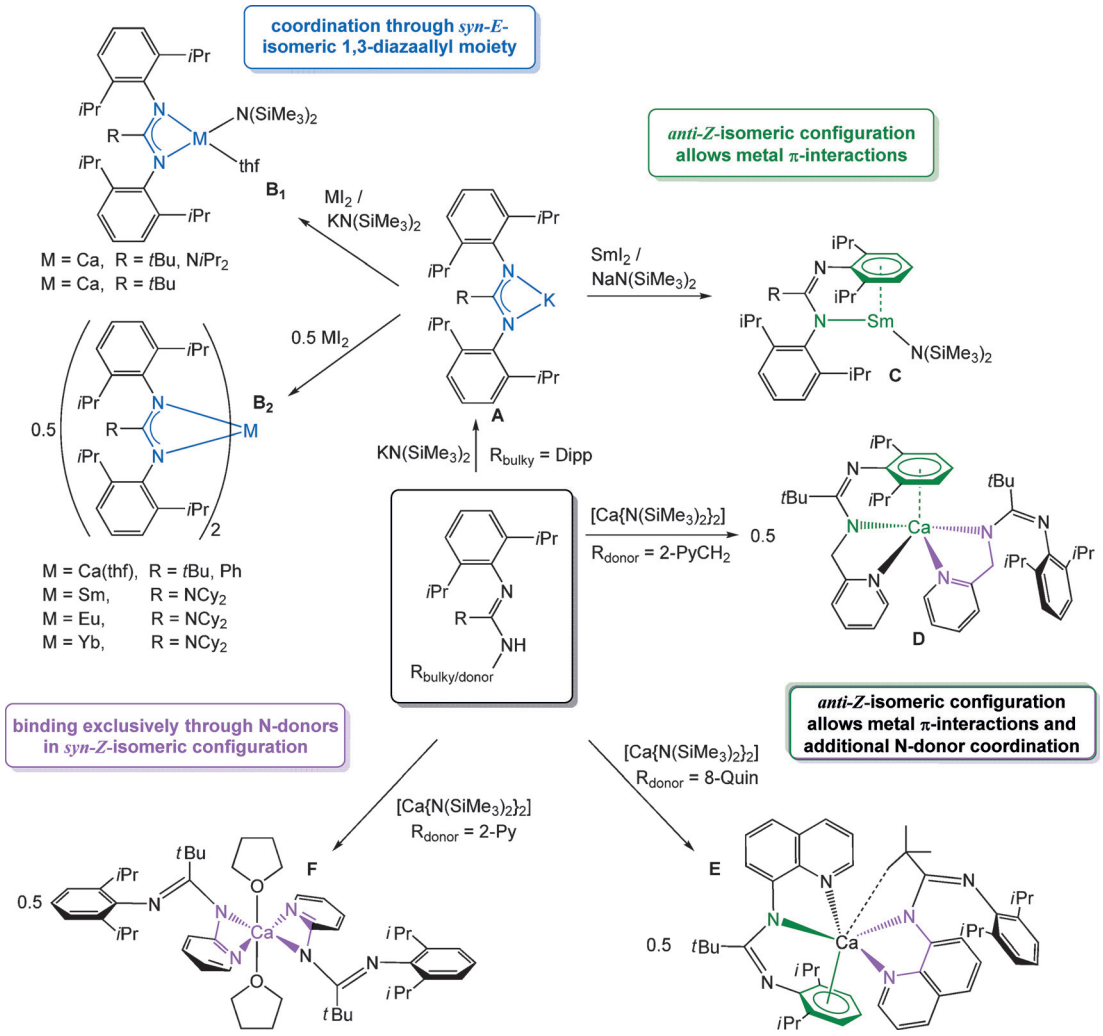

Scheme 2. *N*-(2,6-Diisopropylphenyl)amidinate complexes of the s-block metals and related divalent lanthanoids prepared by salt metathesis or metalation (bottom) reactions from the potassium derivative. The diverse coordination modes are clarified with different colors in accordance with Scheme 1.

plexes $[(thf)_nA\{HN\text{-}C(tBu)=NDipp\}]_\infty$ [A/*n* = Na/2 (**4a**), K/1 (**4b**)] were isolated after filtration, evaporation of the solvent from the filtrate, and recrystallization from a THF solution. Crystal structure determinations of the sodium and potassium derivatives **4a** and **4b** (vide infra) finally verified the liberation of 2-vinylpyridine. In contrast to the reactivity of the alkaline earth metal-based metalation reagents, a β-deprotonation occurred, immediately followed by a deamidation process with release of 2-vinylpyridine. The lifetime of the β-deprotonation intermediate was too short for detection by NMR spectroscopy, but the final products form without any other side products (see Figure S13 in the Supporting Information). Although this two-step process of β-metalation and deamidation is unique in amidinate chemistry of the s-block metals, there are some precedents in the literature employing heterobimetallic superbases. Phenylethyldimethylamine has been quantitatively deprotonated by BuLi/*t*BuOK reagents (Lochmann–Schlosser bases) at the β-position of the N atom leading to a coordination polymer of the thf adduct of 2-dimethylamino-1-phenylethylpotassium at low temperatures that degraded at RT to styrene and dimethylamide ions.[16] Other strong heterobimetallic Li/Zn- and Li/Al-based superbases show comparable reaction patterns, and bridging dimethylamide ions between lithium and zinc as well as lithium and aluminium have been observed (reaction 4).[17]

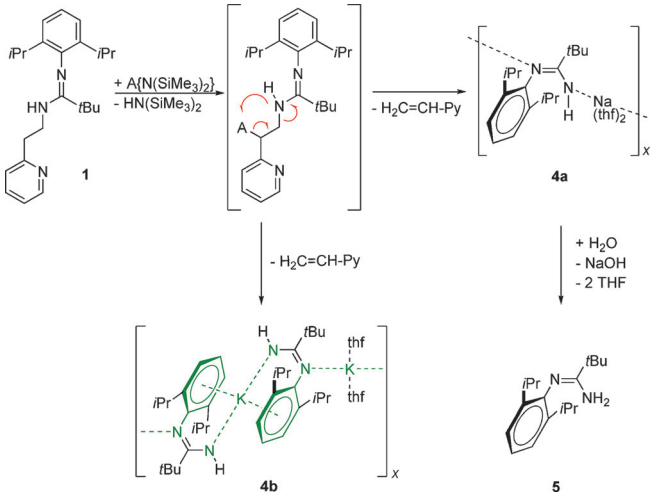

The strikingly different reaction behavior of complexes with the isoelectronic ion pairs Na^+/Mg^{2+} and K^+/Ca^{2+} initiated us to also include the lithium derivative in our investigations. The reaction of $LiN(SiMe_3)_2$ with *N*-(2-pyridylethyl)-*N*′-(2,6-diisopropylphenyl)pivalamidine (**1**) in a mixture of toluene and TMEDA (*N*,*N*,*N*′,*N*′-tetramethylethylenediamine) yielded the metalation product (reaction 5), as also observed for the alkaline earth metal derivatives. Crystal structure determination (vide infra) verified the constitution of the lithium-derived bis(dimethylamino)ethane-(tmeda) adduct **6** . The chemistry of the lithium derivative represents another example of the diagonal relationship in the periodic table because lithiation follows the same reaction pathway as metalation with alkaline earth metal reagents, whereas the heavier alkali metals exhibit a strikingly different reactivity.

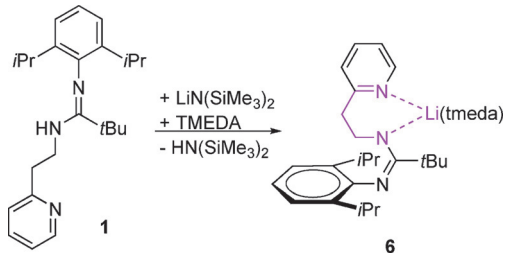

The salt-metathesis reaction of intermediately prepared **4b** with $[(thf)_4CaI_2]$ in tetrahydrofuran yielded complex $[(thf)_4Ca\{HN\text{-}C(tBu)=NDipp\}_2]$ (**7**) according to reaction 6. The insolubility of KI in ethereal solutions avoids the formation of mixed-metal species such as ligated potassium calciates of the type $K[CaR_3]$ or $K_2[CaR_4]$ (as have been observed and structurally identified previously).[18,19] The large number of four bound thf ligands in the isolated and crystalline **7** already indicated that the amidinate anions act as monodentate bases, which was verified by an X-ray structure determination (vide infra).

The unique and unexpected dehydroamination reaction of the heavy alkali metal reagents shown in reaction 4 contrasts

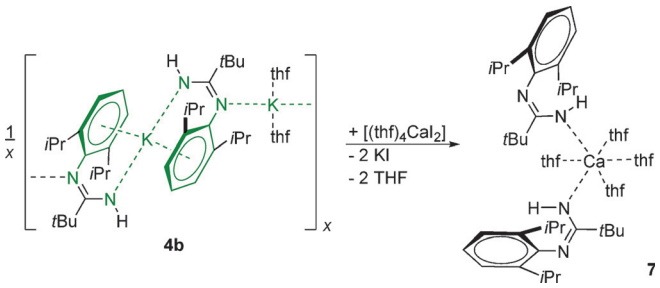

with the reaction of the heavy alkaline earth metal derivatives and of $LiN(SiMe_3)_2$. This deviating behavior seems to be independent of the metalating reagent [KH and $KN(SiMe_3)_2$] and the solvent (THF and toluene), and only a consequence of the softness of the alkali metal ions. Therefore, the value of the surface charge (simply calculated as the quotient of charge and surface of the ion, Li^+ 0.88×10^{-3}, Na^+ 0.69×10^{-3}, K^+ 0.52×10^{-3}, Mg^{2+} 1.85×10^{-3}, Ca^{2+} 1.40×10^{-3}, and Sr^{2+} 1.21×10^{-3} e pm^{-2}) represents the major factor for this deviating behavior of metalation and dehydroamination. Furthermore, intramolecular steric strain in combination with soft alkali metals was also suspected to be responsible for this exceptional reaction behavior. Due to this consideration, we prepared the appropriate *N*-(2-pyridylethyl)-*N*′-(2,6-diisopropylphenyl)formamidine (**8**) from Dipp-NH_2, $HC(OEt)_3$, and 2-$PyCH_2CH_2NH_2$ without solvent at 140 °C according to reaction 7; isolation and purification of intermediately formed Dipp-N=CH-OEt[20,21] gave no significant improvement of the yields. Metalation of formamidine **8** with $AN(SiMe_3)_2$ in toluene yielded the corresponding metalation products $[(thf)A\{HC(=NDipp)(\text{-}NCH_2CH_2Py)\}]_2$ [A = Na (**9a**), K (**9b**)] after recrystallization from THF solution as depicted in reaction 7. Cleavage of the C–N bond and liberation of 2-vinylpyridine were not observed here, verifying the additional relevance of steric pressure induced by the bulky *tert*-butyl group in **1** and the contact to soft alkali metal ions.

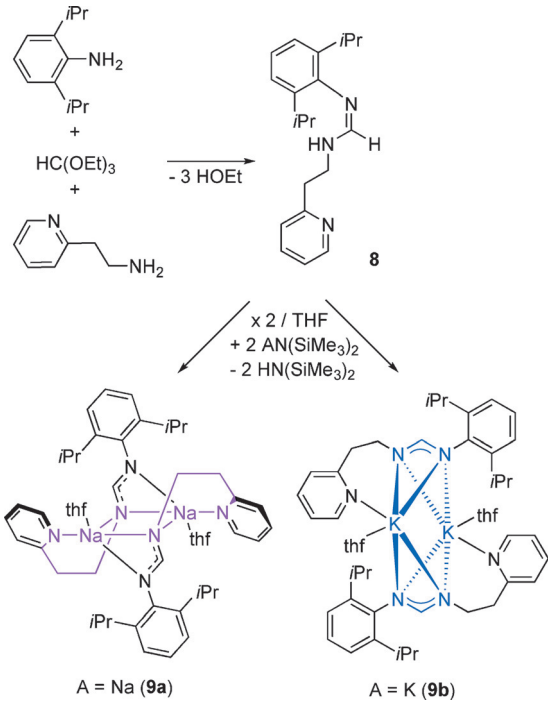

NMR spectroscopy

Selected NMR parameters are summarized in Table 1. Two sets of resonances are observed for magnesium complex **3** and amidine **8**. This finding suggests the presence of two isomeric forms in solution. The carbon atoms C_{NCN} of the amidine and amidinate units in **3** show low-field-shifted resonances; deprotonation enhances these shifts toward even lower field by approximately 15 ppm. Substitution of the 2-pyridylethyl substituent by a hydrogen atom shifts this resonance to a higher field by approximately 10 ppm. Similar effects are also found for the *ipso*-carbon atoms iC_{Dipp} of the 2,6-diisopropylphenyl groups. Small dependencies on the chemical $^{13}C\{^1H\}$ NMR shifts are also observed for the 2-pyridylethyl groups with respect to the coordination of the pyridyl base to the metal ions.

Table 1. Selected ^{1}H and $^{13}C\{^{1}H\}$ NMR data (in ppm) of Dipp-N=C(*t*Bu)-N(H)-C_2H_4-Py (**1**), [{$(Me_3Si)_2N$}Ca{Dipp-N=C(*t*Bu)-N-C_2H_4-Py}] (**2a**), [{$(Me_3Si)_2N$}Sr{Dipp-N=C(*t*Bu)-N-C_2H_4-Py}] (**2b**), [Mg{Dipp-N=C(*t*Bu)-*N*-C_2H_4-Py}$_2$] (**3**), [$(thf)_2$Na{Dipp-N=C(*t*Bu)-N(H)}] (**4a**), [$(thf)_2$K{Dipp-N=C(*t*Bu)-N(H)}] (**4b**), Dipp-N=C(*t*Bu)-NH_2 (**5**), [$(thf)_4$Ca{Dipp-N=C(*t*Bu)-N(H)}$_2$] (**7**), Dipp-N=C(H)-N(H)-C_2H_4-Py (**8**), [(thf)Na{Dipp-N=C(H)-N-C_2H_4-Py}]$_2$ (**9a**), and [(thf)K{Dipp-N=C(H)-N-C_2H_4-Py}]$_2$ (**9b**) (Allred–Rochow electronegativity (EN) of hydrogen and the corresponding s-block metals).

Compound	EN	Solvent	$\delta(C_{NCN})$	$\delta(iC_{Dipp})$	$\delta(C_{CMe3})$	$\delta(C_{NCH2})$	$\delta(C_{CH2Py})$	$\delta(iC_{Py})$
1	2.20 (H)	C_6D_6	157.2	147.7	39.1	43.1	37.1	160.6
2a	1.04 (Ca)	C_6D_6	172.7	156.4	40.1	49.2	39.0	162.4
2b	0.99 (Sr)	C_6D_6	172.2	159.0	39.6	49.7	39.2	162.5
3	1.23 (Mg)	C_6D_6	176.7, 164.5	151.8, 146.9	40.3	49.2, 46.7	40.0, 38.1	165.0, 162.8
4a	1.01 (Na)	C_6D_6	161.1	145.5	37.0	–	–	–
4b	0.91 (K)	C_6D_6	161.1	145.5	37.0	–	–	–
5	2.20 (H)	$CDCl_3$	162.2	144.5	37.1	–	–	–
7	1.04 (Ca)	C_6D_6	161.2	145.6	37.0	–	–	–
8	2.20 (H)	$CDCl_3$	159.8, 158.3	147.7	–	43.9, 39.7	40.8, 37.7	148.8
9a	1.01 (Na)	C_6D_6	170.0	151.4	–	55.9	42.4	163.1
9b	0.91 (K)	$[D_8]$THF	166.5	150.3	–	58.1	44.3	164.1

Molecular structures

To elucidate the steric pressure within these compounds, we also performed X-ray diffraction analysis. The resulting molecular structures and atom number schemes of the amidines **1** and **8** are depicted in Figure 1. Due to poor crystal quality and disorder of part of the molecule, we were only able to obtain a structural motif of **8**; recrystallization efforts from various solvents remained unsuccessful. Despite the fact that discussion of structural parameters is limited, the isomeric structure of **8** was verified. Intramolecular steric strain enforces a *syn-Z*-configuration of **1** stabilized by a N2–H···N3 hydrogen bridge between the amidine and the pyridyl group. In contrast to this intramolecular hydrogen bridge, **8** forms a strand structure through intermolecular N2–H···N1′ bridges (intermolecular N1′···N2 distance: 303.2(5) pm). This kind of aggregation requires an *anti-Z*-isomeric **8** and also explains the flexibility of the 2-pyridylethyl sidearm leading to rather free motion and disordering of this substituent and, thus, to a poor quality of the crystal structure determination.

Molecular structure and atom number scheme of [{$(Me_3Si)_2N$}Ca{*t*BuC(=NDipp)(-NCH_2CH_2Py)}] (**2a**) are shown in Figure 2; the strontium derivative **2b** crystallized isotypic to **2a** and is not represented for simplicity. These complexes exhibit remarkable structural features. The side-on orientation of the Dipp groups allows an effective alkaline earth metal π-interaction with rather small Ca–C (275.0(3)–304.8(3) pm) and Sr–C bond lengths (288.5(3)–309.8(3) pm) leading to distances between the aryl centroid and calcium or strontium atoms of 255.4 and 268.0 pm, respectively. These values are larger than those observed for calciocenes and strontiocenes due to an enhanced electrostatic attraction in such sandwich complexes.[22] The rather low shielding degree of the alkaline earth metal atoms in **2a** and **2b** leads to agostic interactions with methyl groups of the bis(trimethylsilyl)amido ligands (Ca1···C30, 315.7(3) pm and Sr1···C30, 308.4(3) pm) causing significantly different distal and proximal Ae1–N4–Si1 and Ae1–N4–Si2 bond angles. The Ae1–N4 bond lengths lie in characteristic ranges as those also observed for terminally bound $N(SiMe_3)_2$ groups of the corresponding calcium and strontium bis[bis(trimethylsilyl)amides].[23,24] Large Si1–N4–Si2 bond angles and short Si–N4 bonds are characteristic for terminal bis(trimethylsilyl)amido ligands at electropositive metals and are a consequence of intramolecular strain and electrostatic repulsion.[25]

The magnesium cation is significantly harder than the heavier homologous alkaline earth metal ions and, hence, avoids interactions to the soft π-systems of aryl groups. Due to this

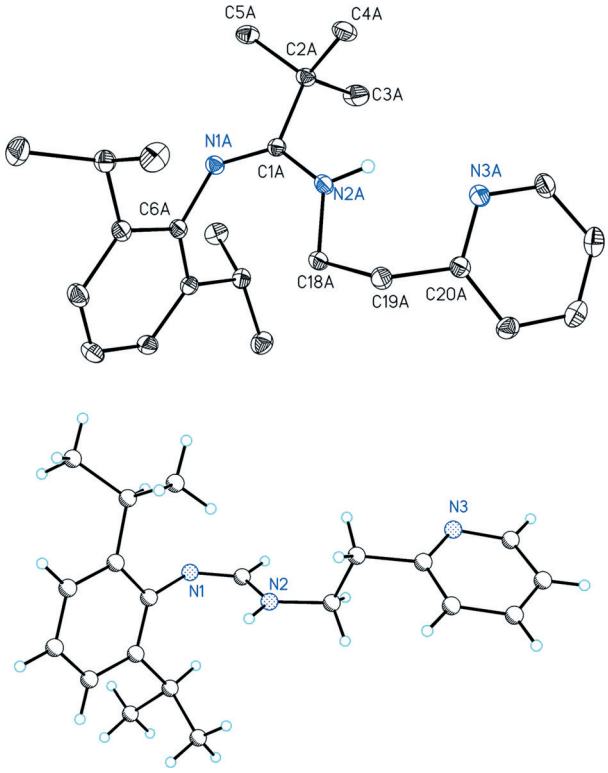

Figure 1. Molecular structures and atom number schemes of the amidines Dipp-N=C(*t*Bu)-N(H)-C_2H_4-Py (**1**, top) and Dipp-N=C(H)-N(H)-C_2H_4-Py (**8**, bottom). The ellipsoids of **1** represent a probability of 30%; the carbon-bound H atoms are neglected for clarity. The atoms of **8** are shown with arbitrary radii due to sub-standard structure determination (see text).

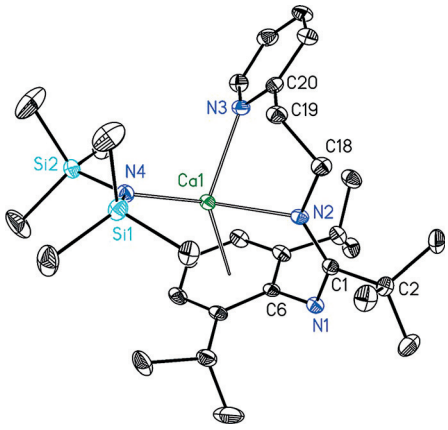

Figure 2. Molecular structure and atom number scheme of heteroleptic [{$(Me_3Si)_2N$}Ca{Dipp-N=C(*t*Bu)-N-C_2H_4-Py}] (**2a**); the strontium congener (**2b**) crystallized isotypic to **2a** and is depicted in Figure S1 in the Supporting Information. The ellipsoids represent a probability of 30%; H atoms are omitted for clarity.

fact, the magnesium atom exclusively binds to the aza-Lewis bases. The molecular structure and atom number scheme of **3** are represented in Figure 3. One ligand acts as a tridentate anion, whereas only two Lewis donors of the other anion bind to the metal atom. Due to this fact and steric requirements, these anions adopt different isomeric forms. The tridentate base binds as a *syn-E* isomer, whereas the bidentate ligand coordinates as a *syn-Z*-isomeric anion. This strikingly different coordination behavior also leads to rather similar C1–N1 and C1–N2 bond lengths, whereas in the other ligand the C25–N5 bond length is significantly smaller than the C25–N4 distance.

The molecular structures and atom number schemes of the alkali metal derivatives **4a** and **4b** are depicted in Figures 4 and 5. The amidinate ligands show different isomeric forms for the sodium (*syn-Z*) and potassium (*anti-Z*) complexes. The preference for the *anti-Z*-isomeric amidinate of the potassium complex **4b** is caused by strong interactions of the alkali metal to the π-systems of the amidinate ligands. In contrast, the sodium ion prefers coordination to hard bases such as tetrahydrofuran or amidinate nitrogen atoms. Both compounds crystallize with strand structures of different shapes. In the sodium derivative **4a**, the tetra-coordinate metal atoms are in distorted tetrahedral environments with rather similar Na–O and Na–N bond lengths and all sodium atoms are in identical crystallo-

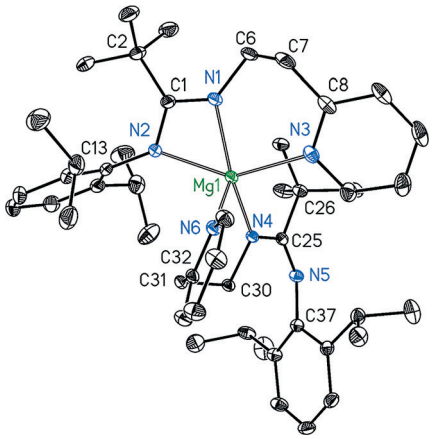

Figure 3. Molecular structure and atom number scheme of [Mg{Dipp-N=C(*t*Bu)-N-C_2H_4-Py}$_2$] (**3**). The ellipsoids represent a probability of 30%; H atoms are omitted.

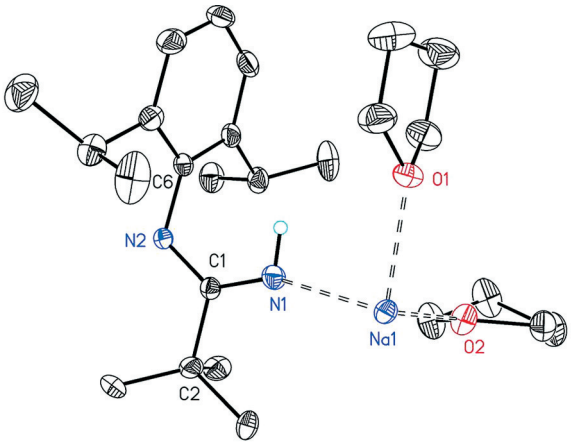

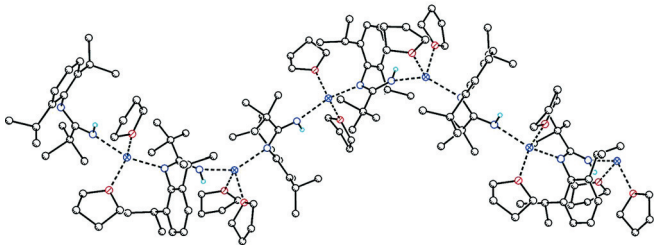

Figure 4. Molecular structure and atom number scheme of the asymmetric unit of [$(thf)_2$Na{Dipp-N=C(*t*Bu)-N(H)}] (**4a**) (top). At the bottom, a part of the strand structure is shown.

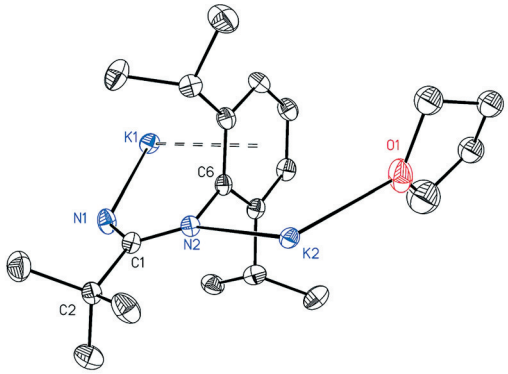

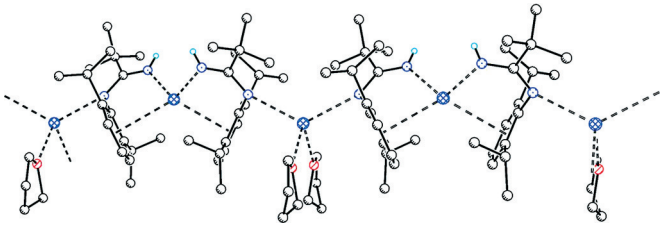

Figure 5. Molecular structure and atom number scheme of the asymmetric unit of [$(thf)_2$K{Dipp-N=C(*t*Bu)-N(H)}] (**4b**) (top). At the bottom, the strand structure is represented; please note that this structure is very different from the chain of the sodium derivative **4a**.

graphic positions. In the strand structure **4b**, two kinds of potassium atoms are present. The atom K1 binds side-on to two aryl groups and two nitrogen bases N1. The other alkali metal atom K2 binds to two crystallographically identical tetrahydrofuran molecules and to the nitrogen bases N2 of two amidinate ions; here the K2–O1 bond length is significantly shorter than the K2–N2 distance.

The molecular structure and atom number scheme of *Z*-isomeric *N*-(2,6-diisopropylphenyl)pivalamidine **5** are represented in Figure 6. The asymmetric unit also contains one ethanol molecule. In the crystalline state, a strand structure is formed through intermolecular N2–H···O_{EtOH} and O_{EtOH}–H···N1 hydrogen bridges. The ethyl group of the ethanol molecule shows a two-site disordering. Both nitrogen atoms of the amidine show sp^2-hybridization and the bond angles lie rather close to 120°. This structure allows a slight π-interaction within the 1,3-diazaallyl fragment, whereas extension of this delocalization into the aryl group seems to be impossible because the aryl group is twisted for steric reasons. Therefore, the N1–C6 single bond of 142.9(2) pm is 8 pm longer than the N2–C1 single bond of the 1,3-diazaallyl moiety.

The lithium derivative **6** crystallizes with two forms in the asymmetric unit (molecules A and B), which are both shown in Figure 7. In both molecules, the lithium atoms bind to the pyridyl moieties and the proximal nitrogen bases of the amidinate units. Furthermore, the coordination spheres are terminated by bidentate tmeda base groups. However, the Lewis acidic metal ions show agostic interactions to the *tert*-butyl group (molecule A, Li1A–C3A, 264.2(4) pm) or to a methylene fragment of the 2-pyridylethyl group (molecule B, Li1B–C19B, 275.6(5) pm).

The molecular structure and atom number scheme of the calcium complex **7** is shown in Figure 8. The hexa-coordinate calcium atom is in a distorted octahedral coordination sphere with the anionic ligands in a *cis* arrangement; due to the bulkiness of the monodentate amidinate ions, a large N1–Ca1–N3 bond angle of 115.46(7)° is observed. The stronger electrostatic attraction here leads to Ca1–N distances that are smaller than the Ca1–O bond lengths.

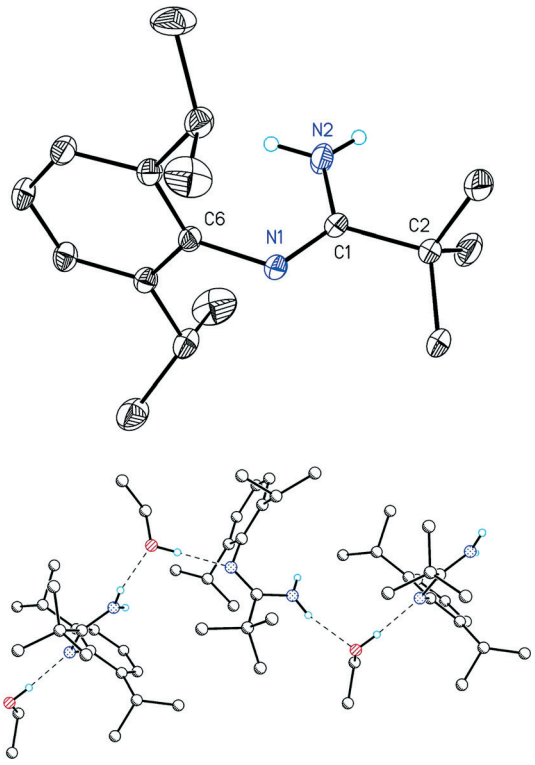

Figure 6. Molecular structure and atom number scheme of Dipp-N=C(*t*Bu)-NH_2 (**5**). The ellipsoids represent a probability of 30%; carbon-bound H atoms are neglected for clarity.

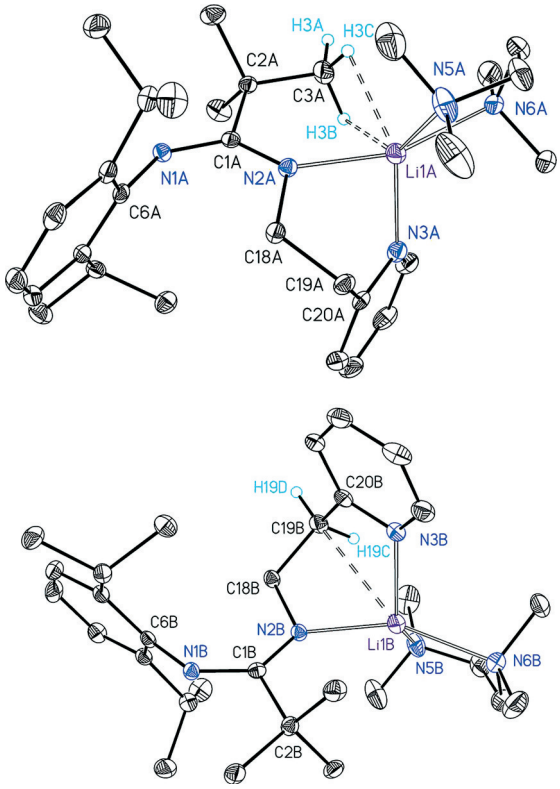

Figure 7. Molecular structures and atom number schemes of the two different molecules of [(tmeda)Li{Dipp-N=C(*t*Bu)-N-C_2H_4-Py}] (**6**). These molecules differ by the agostic interactions to the *tert*-butyl group (top, molecule A) and to the methylene unit of the 2-pyridylethyl group (bottom, molecule B). The ellipsoids represent a probability of 30%; H atoms are only shown for alkyl fragments involved in agostic bondings (dashed lines).

The molecular structures and atom number schemes of the alkali metal complexes **9a** and **9b** are shown in Figure 9. The presence of another Lewis base in the sidearm leads to discrete dinuclear complexes with central four-membered A_2N_2 [A = Na (**9a**), K (**9b**)] rings. These small rings enforce short non-bonding trans-annular A···A contacts of 300.8(1) and 340.86(8) pm for the sodium and potassium derivatives, respectively. Ligated thf molecules complete the coordination spheres of the alkali metals. In both complexes, the penta-coordinate alkali metal atoms prefer the coordination to hard Lewis donors rather than to the soft π-systems of the aryl moieties, which now act as protecting groups at the periphery of the molecules. A sixth coordination site is blocked by the isopropyl group of the Dipp substituent with the smallest Na···Ci_{Pr}

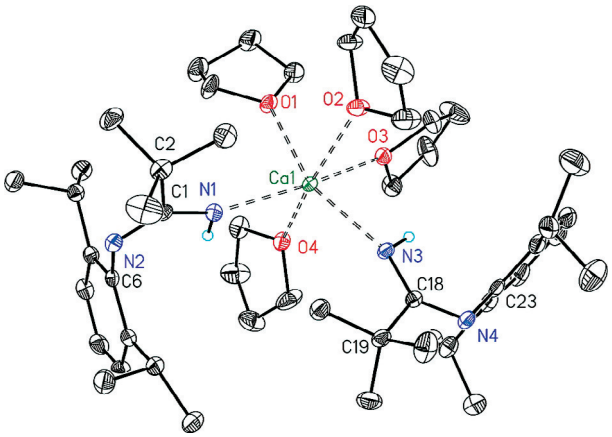

Figure 8. Molecular structure and atom number scheme of [(thf)$_4$Ca{Dipp-N=C(*t*Bu)-N(H)}$_2$] (**7**). The ellipsoids represent a probability of 30%; all carbon-bound H atoms are neglected for clarity.

and K···Ci_{Pr} distances being 357.9(2) and 336.9(3) pm, respectively. The even shorter K···Ci_{Pr} contact clearly suggests agostic bonding and lies on the order of magnitude for K···C π-interactions as observed for the strand structure of **4b**.

To discuss the structural peculiarities of the amidinates (charge delocalization and isomerism) in dependency of the metal (size and hardness) and the substitution pattern, selected bond lengths and angles are listed in Table 2. For comparison reasons, the free amidines **1**, **5**, and **8** are also included. The 1,3-diazaallyl fragments show negligible charge transfer to the attached groups and undisturbed single bonds between sp^2-hybridized carbon and nitrogen atoms (average N_{Dipp}–C_{Dipp} = 140.5 pm) and between sp^3-hybridized carbon and nitrogen atoms (average N_{CH2}–C_{CH2} = 145.9 pm) are observed.

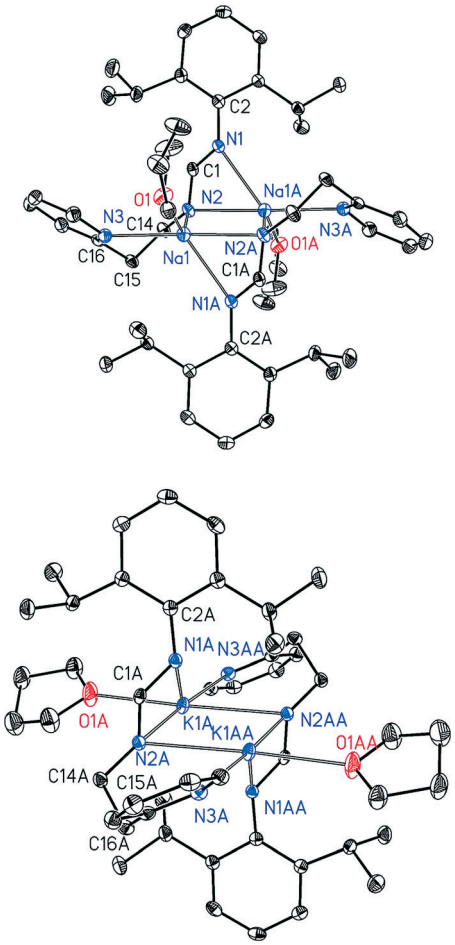

Figure 9. Molecular structures and atom number schemes of the dinuclear complexes [(thf)Na{Dipp-N=C(H)-N-C$_2$H$_4$-Py}]$_2$ (**9a**, top) and [(thf)K{Dipp-N=C(H)-N-C$_2$H$_4$-Py}]$_2$ (**9b**, bottom). The ellipsoids represent a probability of 90%; H atoms are neglected for clarity reasons.

Table 2. Selected bond lengths and angles of Dipp-N=C(*t*Bu)-N(H)-C$_2$H$_4$-Py (**1**), [{(Me$_3$Si)$_2$N}Ca{Dipp-N=C(*t*Bu)-N-C$_2$H$_4$-Py}] (**2a**), [{(Me$_3$Si)$_2$N}Sr{Dipp-N=C(*t*Bu)-N-C$_2$H$_4$-Py}] (**2b**), [Mg{Dipp-N=C(*t*Bu)-N-C$_2$H$_4$-Py}$_2$] (**3**), [(thf)$_2$Na{Dipp-N=C(*t*Bu)-N(H)}] (**4a**), [(thf)$_2$K{Dipp-N=C(*t*Bu)-N(H)}] (**4b**), Dipp-N=C(*t*Bu)-NH$_2$ (**5**), [(tmeda)Li{Dipp-N=C(*t*Bu)-N-C$_2$H$_4$-Py}] (**6**), [(thf)$_4$Ca{Dipp-N=C(*t*Bu)-N(H)}$_2$] (**7**), Dipp-N=C(H)-N(H)-C$_2$H$_4$-Py (**8**), [(thf)Na{Dipp-N=C(H)-N-C$_2$H$_4$-Py}]$_2$ (**9a**), and [(thf)K{Dipp-N=C(H)-N-C$_2$H$_4$-Py}]$_2$ (**9b**).

Compound	M	Isomer	C_{Dipp}–N_{Dipp} [pm]	C_{NCN}–N_{Dipp} [pm]	C_{NCN}–N_{CH2} [pm]	C_{NCN}–C_{tBu} [pm]	N_{CH2}–C_{CH2} [pm]	C_{Dipp}-N_{Dipp}-C_{NCN} [°]	N_{Dipp}-C_{NCN}-N_{CH2} [°]	C_{NCN}-N_{CH2}-C_{CH2} [°]
1	H	*syn-Z*	141.1(2)	127.8(2)	135.9(2)	153.9(2)	145.4(2)	126.7(1)	128.6(1)	128.7(1)
		syn-Z	141.0(2)	128.0(2)	135.8(2)	154.1(2)	145.2(2)	126.1(1)	128.6(1)	130.0(1)
2a	Ca	*syn-Z*	139.6(4)	132.4(4)	135.4(4)	155.0(4)	147.0(4)	116.4(3)	120.9(3)	121.2(3)
2b	Sr	*syn-Z*	139.8(4)	131.7(4)	134.9(4)	155.3(4)	146.2(4)	117.7(3)	121.7(3)	121.0(3)
3	Mg	*syn-E*	141.5(2)	134.0(2)	132.9(2)	155.5(2)	145.0(2)	127.4(1)	110.3(1)	129.4(1)
		syn-Z	139.6(2)	131.1(2)	135.1(2)	155.8(2)	147.5(2)	131.9(1)	130.3(1)	112.7(1)
4a	Na	*syn-Z*	142.0(2)	133.8(2)	131.8(2)	153.6(3)	90(2) (H)	115.8(2)	128.3(2)	110(2) (H)
4b	K	*anti-Z*	140.7(3)	132.2(3)	132.5(3)	154.6(4)	85(3) (H)	116.5(2)	123.8(2)	108(2) (H)
5	H	*Z*	142.9(2)	129.1(2)	134.9(2)	153.0(2)	86(2) (H)	117.8(1)	123.4(1)	119(2), 123(1) (H)
6	Li	*syn-Z*	138.4(3)	131.6(3)	133.9(3)	155.0(3)	146.4(3)	128.7(2)	132.8(2)	117.2(2)
		syn-Z	138.8(3)	131.8(3)	133.9(3)	155.1(3)	146.4(3)	129.8(2)	132.4(2)	117.1(2)
7	Ca	*syn-Z*	140.6(3)	131.6(3)	133.5(3)	154.0(3)	83(3) (H)	118.9(2)	128.5(2)	106(2) (H)
		syn-Z	140.0(3)	131.9(3)	134.2(3)	154.0(3)	88(3) (H)	118.5(2)	127.7(2)	107(2) (H)
8	H[a]	*anti-Z*	143.0(5)	129.0(5)	134.4(5)	–	146.2(5)	119.9(3)	129.0(4)	122.3(4)
9a	Na	*syn-E*	140.2(2)	132.8(2)	131.2(2)	–	145.1(2)	118.6(1)	122.4(1)	116.2(1)
9b	K	*syn-E*	139.1(2)	133.4(2)	130.3(2)	–	144.7(2)	119.7(2)	121.8(2)	116.8(2)
		syn-E	140.1(2)	132.9(3)	131.0(2)	–	145.1(2)	117.4(2)	122.2(2)	116.5(2)

[a] H atom was localized in the difference Fourier synthesis but an isotropic refinement of the parameters was impossible due to poor crystal quality.

Compared with these bond lengths, the 1,3-diazaallyl units show far-reaching charge delocalization and even for the protonated derivatives **1**, **5**, and **8**, the C_{NCN}–N_{CH2} bonds are significantly shorter than a characteristic single bond. As expected, the C_{NCN}–C_{tBu} bonds between the 1,3-diazaallyl fragments and the *tert*-butyl groups are also long.

The bond lengths between the metal (or hydrogen) and the nitrogen bases are listed in Table 3. From the column with the coordination numbers of the s-block metal atoms, it is obvious that these amidinate ligands can adopt diverse coordination modes. The coordination behavior is dominated by intramolecular steric repulsion between the ligands and the tendency of the metal to also form π-interactions with the bulky aryl group. The hard metal ions lithium, sodium, and magnesium avoid such side-on coordination to the Dipp substituents, whereas the softer potassium, calcium, and strontium ions are able to coordinate to the π-systems of the aryl group. In all complexes [including the protonated forms (amidines)], the N_{CH2} bases of the amidinates are part of the coordination spheres of the metals and usually form the smallest M–N distances; only the bis(trimethylsilyl)amido ligands in complexes **2a** and **2b** show shorter Ae–N bonds. This fact together with the observation that the C_{NCN}–N_{Dipp} bond is usually shorter than the C_{NCN}–N_{CH2} bond verifies that the negative charge of the amidinate ion is more expressed on the N_{CH2} base leading to a stronger electrostatic attraction. The bulkiness of the Dipp group often hinders a coordination of the attached nitrogen atom and this group is often turned to the outside of the complex.

Steric requirements as discussed above also lead to distortion of the amidinate backbone (Table 2). The bond angles seem to be quite flexible and the N_{Dipp}–C_{NCN}–N_{CH2} values vary between 110.3(1)° for **3** and 132.8(2)° for **6**. Similar observations are also true for the angles at the nitrogen atoms of the amidinate ions.

Summary and Conclusions

We have demonstrated that the softness of the s-block metals play a peculiar role when pivalamidine (**1**) is reacted with s-block metal bases. The soft sodium and potassium bis(trimethylsilyl)amides lead to a β-deprotonation reaction immediately followed by a deamidation process yielding the complexes $[(thf)_2Na\{Dipp\text{-}N{=}C(tBu)\text{-}N(H)\}]$ (**4a**) and $[(thf)_2K\{Dipp\text{-}N{=}C(tBu)\text{-}N(H)\}]$ (**4b**) as well as 2-vinylpyridine, whereas the lighter (and harder) lithium bis(trimethylsilyl)amide deprotonates this amidine and $[(tmeda)Li\{Dipp\text{-}N{=}C(tBu)\text{-}N\text{-}C_2H_4\text{-}Py\}]$ (**6**) is formed after addition of TMEDA. This strikingly different reaction behavior also initiated the investigation of this reaction with alkaline earth metal-based metalation reagents. According to the diagonal relationship in the periodic table, only deprotonation is observed, yielding the pivalamidinates of magnesium, $[Mg\{Dipp\text{-}N{=}C(tBu)\text{-}N\text{-}C_2H_4\text{-}Py\}_2]$ (**3**), calcium, and strontium, $[\{(Me_3Si)_2N\}Ae\{Dipp\text{-}N{=}C(tBu)\text{-}N\text{-}C_2H_4\text{-}Py\}]$ with Ae being Ca (**2a**) and Sr (**2b**), as also found for the lithiation reaction. Nevertheless, the metathetical approach of **4b** with calcium diiodide also allows the synthesis of the calcium derivative $[(thf)_4Ca\{Dipp\text{-}N{=}C(tBu)\text{-}N(H)\}_2]$ (**7**) with the dehydroaminated ligand. The protonated form, $Dipp\text{-}N{=}C(tBu)\text{-}NH_2$ (**5**), contains an amino group, suggesting that the Dipp-bound nitrogen atom is less basic than the other one. This is in agreement with those derivatives with a 2-pyridylethyl group attached to this nitrogen atom [derivatives $Dipp\text{-}N{=}C(tBu)\text{-}N(H)\text{-}C_2H_4\text{-}Py$ (**1**) and $Dipp\text{-}N{=}C(H)\text{-}N(H)\text{-}C_2H_4\text{-}Py$ (**8**)]. Less strained formamidine

Table 3. Selected bond lengths (pm) of $Dipp\text{-}N{=}C(tBu)\text{-}N(H)\text{-}C_2H_4\text{-}Py$ (**1**), $[\{(Me_3Si)_2N\}Ca\{Dipp\text{-}N{=}C(tBu)\text{-}N\text{-}C_2H_4\text{-}Py\}]$ (**2a**), $[\{(Me_3Si)_2N\}Sr\{Dipp\text{-}N{=}C(tBu)\text{-}N\text{-}C_2H_4\text{-}Py\}]$ (**2b**), $[Mg\{Dipp\text{-}N{=}C(tBu)\text{-}N\text{-}C_2H_4\text{-}Py\}_2]$ (**3**), $[(thf)_2Na\{Dipp\text{-}N{=}C(tBu)\text{-}N(H)\}]$ (**4a**), $[(thf)_2K\{Dipp\text{-}N{=}C(tBu)\text{-}N(H)\}]$ (**4b**), $Dipp\text{-}N{=}C(tBu)\text{-}NH_2$ (**5**), $[(tmeda)Li\{Dipp\text{-}N{=}C(tBu)\text{-}N\text{-}C_2H_4\text{-}Py\}]$ (**6**), $[(thf)_4Ca\{Dipp\text{-}N{=}C(tBu)\text{-}N(H)\}_2]$ (**7**), $Dipp\text{-}N{=}C(H)\text{-}N(H)\text{-}C_2H_4\text{-}Py$ (**8**), $[(thf)Na\{Dipp\text{-}N{=}C(H)\text{-}N\text{-}C_2H_4\text{-}Py\}]_2$ (**9a**) and of $[(thf)K\{Dipp\text{-}N{=}C(H)\text{-}N\text{-}C_2H_4\text{-}Py\}]_2$ (**9b**) (C.N.(M) coordination number of the metal).

Compound	M	Isomer	C.N.(M)	$M\text{–}N_{Dipp}$	$M\text{–}N_{CH2}$	$M\text{–}N_{Py}$	$M\text{–}N_{NSi2}$
1	H	*syn-Z*	–[a]	–	87 (2) (H)	–	–
		syn-Z	–[a]	–	87 (2) (H)	–	–
2a	Ca	*syn-Z*	3+6[b]	–	238.5(3)	245.5(3)	230.4(3)
2b	Sr	*syn-Z*	3+6[b]	–	254.0(3)	259.6(3)	244.5(3)
3	Mg	*syn-E*	5	221.0(1)	205.2(1)	230.7(1)	–
		syn-Z	5	–	211.4(1)	216.5(1)	–
4a	Na	*syn-Z*	4	237.8(2)	233.5(2)	–	–
4b	K	*anti-Z*	4/2+12[c]	274.4(2)	275.0(2)	–	–
5	H	*Z*	–[d]	–	87 (2) (H)	–	–
6	Li	*syn-Z*	4	–	204.5(4)	212.5(4)	–
		syn-Z	4	–	203.1(4)	213.9(5)	–
7	Ca	*syn-Z*	6	–	236.5(2)	–	–
		syn-Z	6	–	236.5(2)	–	–
8	H	*anti-Z*	–[d]	–	88 (H)[e]	–	–
9a	Na	*syn-E*	5	246.9(1)	245.5(1), 251.6(1)	247.2(1)	–
9b	K	*syn-E*	5	280.0(2)	282.8(2), 283.4(2)	284.6(2)	–
		syn-E	5	289.5(2)	282.3(2), 282.5(2)	293.1(2)	–

[a] Intramolecular N_{CH2}–H···N_{Py} hydrogen bridge. [b] The Ae metals bind to three nitrogen bases and six carbon atoms of the aryl group; the agostic interactions are neglected. [c] Two K atoms in different coordination spheres with one K binding to two N bases and side-on to two aryl groups. [d] Intermolecular hydrogen bridge. [e] H atom was localized in the difference Fourier synthesis but an isotropic refinement of the parameters was impossible due to poor crystal quality.

Dipp-N=C(H)-N(H)-C_2H_4-Py (**8**) can be metalated at the form-amidine functionality by sodium or potassium bis(trimethylsilyl)amide, yielding the corresponding dinuclear complexes [(thf)Na{Dipp-N=C(H)-N-C_2H_4-Py}]$_2$ (**9a**) or [(thf)K{Dipp-N=C(H)-N-C_2H_4-Py}]$_2$ (**9b**), respectively. This finding verifies that the dehydroamination reaction requires steric pressure and that lack of strain leads to the expected metalation reaction of the amidine unit and finally to the complexes **9a** and **9b**. This reaction pattern is presented in Scheme 3.

In all of these compounds, the charge delocalization is limited to the 1,3-diazaallyl unit. The bulky Dipp group is turned out of the allyl plane hindering effective π-interaction with this aromatic substituent. The Dipp-bound nitrogen atom N_{Dipp} is sterically shielded and less negative than the other allyl nitrogen base N_{CH2} and therefore, the hydrogen atoms in amidines and the s-block metal ions in their amidinates always bind to this aza-base. In addition, the hydrogen atoms in amidines form either intra- or intermolecular hydrogen bridges. The metal additionally coordinates to the pyridyl group or to N_{Dipp} and the soft metal ions K^+, Ca^{2+}, and Sr^{2+} also tend to show π-interactions with the side-on bound aryl groups. In summary, these bulky ligands show a diverse coordination chemistry to s-block metals and even a surprising reactivity with metalation reagents depending on the softness of the metal and the bulkiness of the ligand.

Experimental Section

General considerations: All manipulations were carried out under a nitrogen atmosphere using standard Schlenk techniques. The solvents THF and toluene were dried over KOH and subsequently distilled over sodium/benzophenone under a nitrogen atmosphere prior to use. Deuterated solvents were dried over sodium, degassed, and saturated with nitrogen. The yields given are not opti-

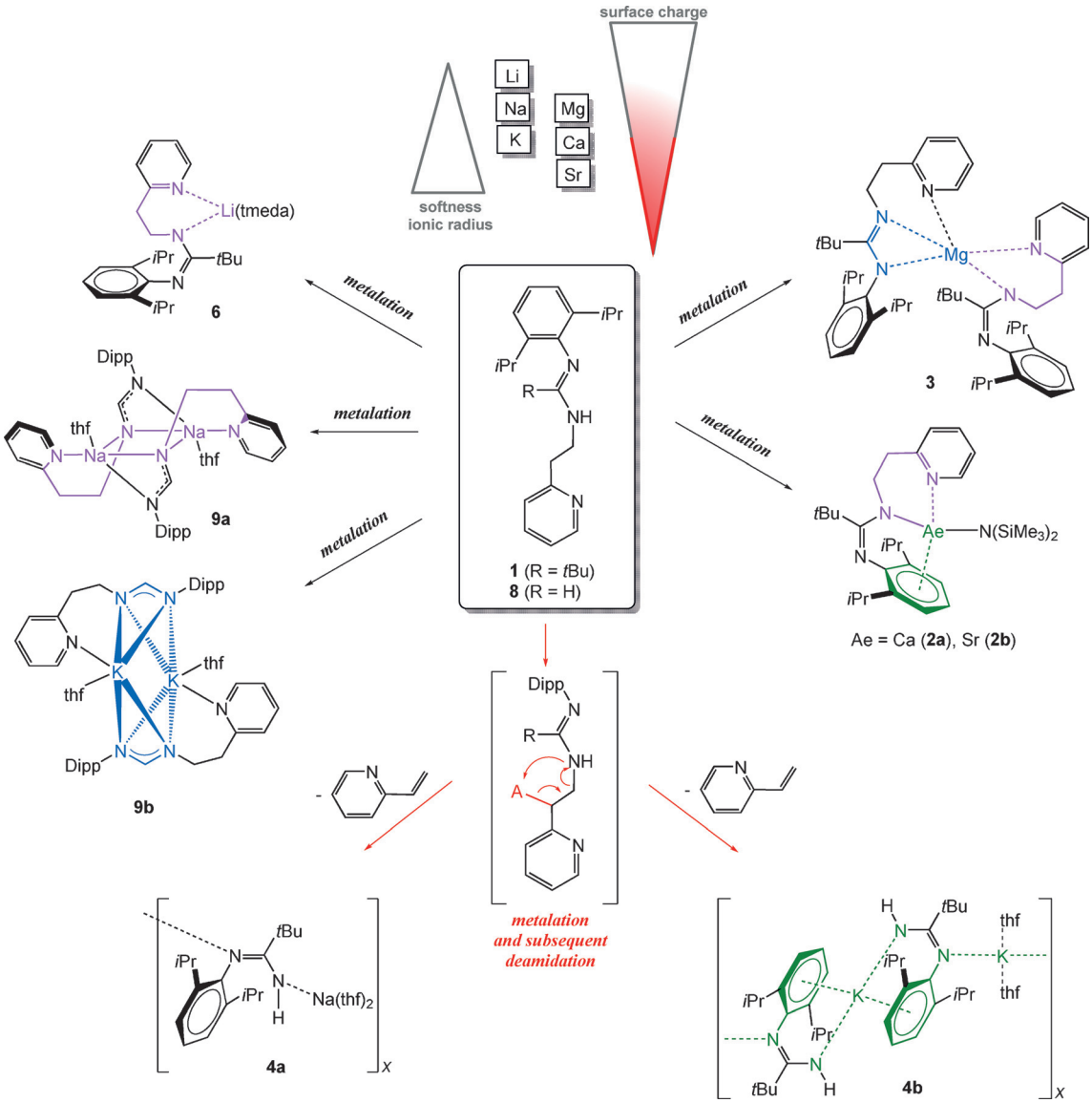

Scheme 3. Bases with soft metal ions and overcrowded amidines enforce dehydroamination of the amidines (red arrows at the bottom), whereas bases with harder metal ions or lack of steric pressure lead to the expected metalating reactions (black arrows), yielding the corresponding amidinates.

mized. ^{1}H and $^{13}C\{^{1}H\}$ NMR spectra were recorded on Bruker Avance 200, Avance 400, and Avance 600 spectrometers. For multiplets the chemical shifts refer to the centers of the signals, ranges are only given for overlapping resonances. All NMR spectra are shown in the Supporting Information. Chemical shifts are reported in parts per million. In some cases ^{1}H-$^{13}C\{^{1}H\}$ HSQC, ^{1}H-$^{13}C\{^{1}H\}$ HMBC, and H-H COSY NMR experiments were performed for the assignment of the resonances. For mass spectrometric investigations, the spectrometers ThermoFinnigan MAT95XL and Finnigan SSQ710 were at our disposal. IR spectra were recorded with a Bruker ALPHA FT-IR spectrometer. Starting $[(thf)_2Ca\{N(SiMe_3)_2\}_2]$ and $[(thf)_2Sr\{N(SiMe_3)_2\}_2]$ were prepared according to literature protocols.[23c,26]

Synthesis of *N*-(2,6-diisopropylphenyl)-*N*′-(2-pyridylethyl)pivalamidine (Dipp-N=C(*t*Bu)-N(H)-C_2H_4-Py) (1): Dipp-NH_2 (9.4 mL, 50.0 mmol) in 40 mL of anhydrous pyridine and pivaloyl chloride (6.2 mL, 50.0 mmol) gave 12.34 g (47.2 mmol, 94%) of Dipp-N(H)CO(*t*Bu). The purity of the product was monitored by use of NMR spectroscopy. The reaction of Dipp-N(H)CO(*t*Bu) (12.0 g, 45.9 mmol) with $SOCl_2$ (11.0 mL, 151.6 mmol) yielded 11.63 g (41.6 mmol, 91%) of pure Dipp-N=C(*t*Bu)Cl. To a toluene (15 mL) solution of $NH_2C_2H_4$-Py (1.18 g, 10.6 mmol) was added dropwise Dipp-N=C(*t*Bu)Cl (2.99 g, 10.6 mmol) at room temperature (RT). The reaction mixture was stirred at 150 °C for 24 h to give a clear pale brown solution. Subsequently, all volatiles were removed in vacuo. The remaining solid was dissolved in 100 mL of dichloromethane and washed two times with aqueous Na_2CO_3 solution (50 mL, 2%). After removal of the solvent, the precipitate was recrystallized from *n*-pentane yielding 2.47 g of **1** (64%). M.p. 58–60 °C; ^{1}H NMR (400.13 MHz, $CDCl_3$, 298.0 K): δ 8.48 (m, 1H, Py N-C*H*), 7.56 (td, $^{3}J_{HH}=7.7$ Hz, $^{4}J_{HH}=1.8$ Hz, 1H, Py *m*-C*H*), 7.12 (m, 1H, Py *p*-C*H*), 6.98 (m, 2H, Dipp *m*-C*H*), 6.94 (m, 1H, Py *o*-C*H*), 6.89 (m, 1H, Dipp *p*-C*H*), 5.61 (broad, 1H, N*H*), 3.01–2.93 (m, 4H, $CH(CH_3)_2$, N-CH_2-), 2.67 (m, 2H, Py-CH_2-), 1.27 (s, 9H, $C(CH_3)_3$), 1.16–1.15 ppm (m, 12H, $CH(CH_3)_2$); ^{13}C NMR (100.62 MHz, $CDCl_3$, 298.0 K): δ 159.9 (Py *i*-*C*), 157.4 (^{q}C), 149.1 (Py N-*C*H), 147.0 (Dipp *i*-*C*), 137.6 (Dipp *o*-*C*), 136.8 (Py *m*-*C*), 123.1 (Py *o*-*C*), 122.0 (Dipp *m*-*C*), 121.7 (Py *p*-*C*), 120.8 (Dipp *p*-*C*), 42.7 (N-CH_2-), 38.8 ($C(CH_3)_3$), 37.6 (Py-CH_2-), 29.2 ($C(CH_3)_3$), 28.4 ($CH(CH_3)_2$), 23.2/22.6 ppm ($CH(CH_3)_2$); ^{1}H NMR (600.15 MHz, C_6D_6, 297.0 K): δ 8.23 (m, 1H, Py N-C*H*), 7.18 (m, 2H, Dipp *m*-C*H*), 7.10 (m, 1H, Dipp *p*-C*H*), 6.91 (td, $^{3}J_{HH}=7.7$ Hz, $^{4}J_{HH}=1.7$ Hz, 1H, Py *m*-C*H*), 6.51 (m, 1H, Py *p*-C*H*), 6.40 (d, $^{3}J_{HH}=7.7$ Hz, 1H, Py *o*-C*H*), 6.11 (broad, 1H, N*H*), 3.29 (sept, $^{3}J_{HH}=6.6$ Hz, 2H, $CH(CH_3)_2$), 3.04 (m, 2H, N-CH_2-), 2.30 (t, $^{3}J_{HH}=6.0$ Hz, 2H, Py-CH_2-), 1.39 (s, 9H, $C(CH_3)_3$), 1.32 ppm (m, 12H, $CH(CH_3)_2$); ^{13}C NMR (150.91 MHz, C_6D_6, 297.0 K): δ 160.6 (Py *i*-*C*), 157.2 (^{q}C), 149.0 (Py N-*C*H), 147.7 (Dipp *i*-*C*), 137.7 (Dipp *o*-*C*), 136.4 (Py *m*-*C*), 128.4 (Dipp *m*-*C*), 123.0 (Dipp *p*-*C*), 122.4 (Py, *o*-*C*), 121.4 (Py *p*-*C*), 43.1 (N-CH_2-), 39.1 ($C(CH_3)_3$), 37.1 (Py-CH_2-), 29.4 ($C(CH_3)_3$), 28.9 ($CH(CH_3)_2$), 23.6/22.6 ppm ($CH(CH_3)_2$); MS (DEI): *m/z* (%) 365 (20, $[M]^+$), 322 (20, $[C_{21}H_{28}N_3]^+$), 308 (10, $[C_{20}H_{26}N_3]^+$), 244 (10, $[C_{16}H_{24}N_2]^+$; $[C_{17}H_{27}N]^+$), 229 (30, $[C_{15}H_{21}N_2]^+$; $[C_{16}H_{23}N]^+$), 186 (20, $[C_{13}H_{16}N]^+$; $[C_{13}H_{16}N]^+$), 146 (20, $[C_{11}H_{14}]^+$; $[C_{10}H_{12}N]^+$), 121 (20, $[C_7H_9N_2]^+$), 106 (100, $[C_7H_8N]^+$), 93 (60, $[C_6H_7N]^+$), 78 (20, $[C_5H_4N]^+$), 57 (60, $[C_3H_7N]^+$), 43 (20, $[C_3H_7]^+$), 41 (30, $[C_2H_3N]^+$). IR (pure): $\tilde{\nu}=3498$ (w), 3395 (w), 3324 (w), 3055 (w), 2957 (w), 2924 (w), 2863 (w), 1650 (w), 1586 (w), 1532 (w), 1469 (w), 1429 (w), 1258 (w), 1229 (w), 1095 (w), 1009 (w), 770 (w), 724 (w), 550 (vw), 502 cm^{-1} (vw); elemental analysis (%) calcd for $C_{24}H_{35}N_3$ (365.55 g mol^{-1}): C, 78.85; H 9.65; N 11.49; found: C, 78.20; H, 9.87; N, 11.14.

Synthesis of [{$(Me_3Si)_2N$}Ca{Dipp-N=C(*t*Bu)-N-C_2H_4-Py}] (2a): A solution of amidine **1** (130 mg, 0.35 mmol) in toluene (8 mL) was added to a solution of $[(thf)_2Ca\{N(SiMe_3)_2\}_2]$ (270 mg, 0.53 mmol) in toluene (8 mL) at RT and the reaction mixture was stirred at RT for 3.5 h. Thereafter, all volatiles were removed in vacuo and 117 mg of **2a** (59%) were isolated as orange crystals after recrystallization from toluene. Physical data show a 6% contamination by $[(thf)_2Ca\{N(SiMe_3)_2\}_2]$. M.p. 156–158 °C (dec.); ^{1}H NMR (400.13 MHz, C_6D_6, 297.0 K): δ 7.87 (m, 1H, Py N-C*H*), 7.17 (m, 2H, Dipp *m*-C*H*), 6.95–6.87 (m, 2H, Py *m*-C*H*, Dipp *p*-C*H*), 6.48–6.43 (m, 2H, Py *p*-C*H*, Py *o*-C*H*), 3.74 (m, 2H, N-CH_2-), 3.59 (m, 2H, thf O-CH_2-), 3.17 (sept, $^{3}J_{HH}=6.8$ Hz, 2H, $CH(CH_3)_2$), 2.84 (m, 2H, Py-CH_2-), 1.44 (s, 9H, $C(CH_3)_3$), 1.30 (d, $^{3}J_{HH}=6.8$ Hz, 7H, $CH(CH_3)_2$), 1.07 (d, $^{3}J_{HH}=6.8$ Hz, 5H, $CH(CH_3)_2$), 0.36 (s, 2H, $[(thf)_2Ca\{N(SiMe_3)_2\}_2]$, $Si(CH_3)_3$), 0.31 (s, 18H, $Si(CH_3)_3$), 0,10 ppm (s, 4H, $HN\{Si(CH_3)_3\}_2$); ^{13}C NMR (100.63 MHz, C_6D_6, 300.0 K): δ 172.7 (^{q}C), 162.4 (Py *i*-*C*), 156.4 (Dipp *i*-*C*), 147.3 (Py N-*C*H), 143.2 (Dipp *o*-*C*), 138.7 (Py *m*-*C*), 124.9 (Py *o*-*C*), 124.1 (Dipp *m*-*C*), 121.3 (Py *p*-*C*), 120.4 (Dipp *p*-*C*), 69.3 (thf, O-CH_2-), 49.2 (N-CH_2-), 40.1 ($C(CH_3)_3$), 39.0 (Py-CH_2-), 30.6 ($C(CH_3)_3$), 28.7 ($CH(CH_3)_2$), 25.2 (thf, -CH_2-), 23.5/21.9 ($CH(CH_3)_2$), 5.9 ($Si(CH_3)_3$), 2.7 ppm ($HN\{Si(CH_3)_3\}_2$); MS (DEI): *m/z* (%) 564 (2, $[M]^+$), 521 (10, $[M-C_3H_7]^+$), 365 (40, $[L]^+$), 322 (45, $[C_{21}H_{28}N_3]^+$), 308 (20, $[C_{20}H_{26}N_3]^+$), 260 (10, $[C_{17}H_{28}N_2]^+$) 244 (25, $[C_{16}H_{23}N_2]^+$; $[C_{17}H_{27}N]^+$), 229 (90, $[C_{16}H_{23}N]^+$; $[C_{15}H_{21}N_2]^+$), 203 (45, $[C_{13}H_{19}N_2]^+$), 186 (35, $[C_{12}H_{14}N_2]^+$; $[C_{13}H_{16}N]^+$), 162 (40, $[C_{10}H_{14}N_2]^+$; $[C_{11}H_{16}N]^+$), 146 (100, $[C_{11}H_{14}]^+$; $[C_{10}H_{12}N]^+$), 130 (35, $[C_9H_8N]^+$), 106 (95, $[C_7H_8N]^+$), 57 (10, $[C_3H_7N]^+$); MS (Micro-ESI pos. in THF and MeOH): *m/z* (%) 366 (<1, $[L+H]^+$), 261 (3, $[C_7H_{11}N]^+$), 244 (100, $[C_{16}H_{24}N_2]^+$; $[C_{17}H_{27}N]^+$), 188 (18, $[C_{12}H_{16}N_2]^+$; $[C_{13}H_{18}N]^+$), 146 (5, $[C_{11}H_{14}]^+$; $[C_{10}H_{12}N]^+$); IR (pure): $\tilde{\nu}=3325$ (vw), 3055 (vw), 2955 (w), 2863 (w), 1655 (m), 1586 (w), 1534 (w), 1469 (w), 1437 (w), 1381 (w), 1360 (w), 1341 (w), 1312 (w), 1289 (w), 1257 (w), 1231 (w), 1104 (w), 1071 (w), 1032 (w), 1011 (w), 933 (w), 879 (w), 813 (w), 784 (m), 747 (m), 681 (w), 657 cm^{-1} (w); elemental analysis (%) calcd for $C_{30}H_{52}CaN_4Si_2$, 565.01 g mol^{-1}): C 63.77, H 9.28, N 9.92; found: C 63.55, H 9.24, N 9.74.

Synthesis of [{$(Me_3Si)_2N$}Sr{Dipp-N=C(*t*Bu)-N-C_2H_4-Py}] (2b): A solution of amidine **1** (62 mg, 0.17 mmol) in toluene (2 mL) was added to a solution of $[(thf)_2Sr\{N(SiMe_3)_2\}_2]$ (94 mg, 0.17 mmol) in toluene (3 mL) at RT and the reaction mixture was stirred at RT for 4 h. Thereafter, all volatiles were removed in vacuo and 67 mg of **2b** (64%) were isolated as yellow crystals after recrystallization from toluene. The same procedure using amidine **1** (146 mg, 0.4 mmol) and $[(thf)_2Sr\{N(SiMe_3)_2\}_2]$ (440 mg, 0.8 mmol) in toluene (20 mL) also led to the formation of **2b** (110 mg, 18%). M.p. 149–153 °C (dec.); ^{1}H NMR (400.13 MHz, C_6D_6, 297.0 K): δ 7.75 (m, 1H, Py N-C*H*), 7.08 (m, 2H, Dipp *m*-C*H*), 6.87–6.83 (m, 2H, Py *m*-C*H*, Dipp *p*-C*H*), 6.44–6.42 (m, 2H, Py *p*-C*H*, Py *o*-C*H*), 3.80 (m, 2H, N-CH_2-), 3.18 (sept, $^{3}J_{HH}=6.8$ Hz, 2H, $CH(CH_3)_2$), 2.69 (m, 2H, Py-CH_2-), 1.54 (s, 9H, $C(CH_3)_3$), 1.25 (d, $^{3}J_{HH}=6.8$ Hz, 6H, $CH(CH_3)_2$), 1.00 (d, $^{3}J_{HH}=6.8$ Hz, 6H, $CH(CH_3)_2$), 0.32 (s, 18H, $Si(CH_3)_3$), 0.10 ppm (s, 3H, $HN\{Si(CH_3)_3\}_2$); ^{13}C NMR (100.61 MHz, C_6D_6, 297.0 K): δ 172.2 (^{q}C), 162.5 (Py *i*-*C*), 159.0 (Dipp *i*-*C*), 146.9 (Py N-*C*H), 144.3 (Dipp *o*-*C*), 138.5 (Py *m*-*C*), 124.8 (Py *o*-*C*), 124.3 (Dipp *m*-*C*), 121.5 (Py *p*-*C*), 119.7 (Dipp *p*-*C*), 49.7 (N-CH_2-), 39.6 ($C(CH_3)_3$), 39.2 (Py-CH_2-), 30.8 ($C(CH_3)_3$), 28.7 ($CH(CH_3)_2$), 23.3/21.9 ($CH(CH_3)_2$), 5.8 ($Si(CH_3)_3$), 2.7 ppm ($HN\{Si(CH_3)_3\}_2$); MS (DEI): *m/z* (%) 365 (75, $[L]^+$), 322 (70, $[C_{21}H_{28}N_3]^+$), 308 (20, $[C_{20}H_{26}N_3]^+$), 259 (5, $[C_{17}H_{27}N_2]^+$) 244 (20, $[C_{16}H_{23}N_2]^+$; $[C_{17}H_{27}N]^+$), 229 (100, $[C_{16}H_{23}N]^+$; $[C_{15}H_{21}N_2]^+$), 186 (20, $[C_{12}H_{14}N_2]^+$; $[C_{13}H_{16}N]^+$), 146 (15, $[C_{11}H_{14}]^+$; $[C_{10}H_{12}N]^+$), 106 (10, $[C_7H_8N]^+$), 58 (2, $[C_3H_6N]^+$); MS (Micro-ESI pos. in THF+MeOH): *m/z* (%) 366 (60, $[L+H]^+$), 261 (3, $[C_7H_{11}N]^+$), 244 (100, $[C_{16}H_{24}N_2]^+$; $[C_{17}H_{27}N]^+$); IR (pure): $\tilde{\nu}=3366$ (vw), 3053 (vw), 2950 (w), 2866 (w), 1651 (w), 1599 (w), 1529 (w), 1477 (w), 1435 (w), 1392 (w), 1355 (w), 1341 (w), 1311 (w), 1246 (w), 1234 (w), 1102 (w), 1063 (m), 1010 (w), 932 (w), 878 (w), 813 (m), 791 (m), 748 (m), 659 (w),

638 cm^{-1} (w); elemental analysis (%) calcd for $C_{30}H_{52}SrN_4Si_2$ (612.55 g mol^{-1}): C, 58.82; H 8.56; N 9.15; found: C, 59.03; H, 8.41; N, 9.05.

Synthesis of [Mg{Dipp-N=C(*t*Bu)-N-C_2H_4-Py}$_2$] (3): To a solution of amidine **1** (366 mg, 1.0 mmol) in *n*-pentane (10 mL) was added 1.1 mL of a 1 M Mg(*n*Bu)$_2$ solution in *n*-heptane at 0 °C and this reaction mixture was stirred at RT for 24 h. During this time, formation of a pale yellow solid was observed. Toluene was added successively to get a clear solution, and after several days, 234 mg of **3** (31 %) were isolated. M.p. > 350 °C; ^{1}H NMR (400.13 MHz, C_6D_6, 297.3 K): δ 8.30 (d, $^3J_{HH}$ = 4.6 Hz, 1 H, Py N-C*H*), 7.76 (m, 1 H, Py N-C*H*), 7.05 (t, $^3J_{HH}$ = 7.5 Hz, 1 H, Dipp *p*-C*H*), 7.01 (t, $^3J_{HH}$ = 7.5 Hz, 1 H, Dipp *p*-C*H*), 6.90–7.27 (m, 4 H, Dipp *m*-C*H*), 6.87 (m, 1 H, Py *m*-C*H*), 6.66 (m, 1 H, Py *p*-C*H*), 6.63 (td, $^3J_{HH}$ = 7.7 Hz, $^4J_{HH}$ = 1.7 Hz, 1 H, Py *m*-C*H*), 6.55 (d, $^3J_{HH}$ = 7.7 Hz, 1 H, Py *o*-C*H*), 6.18 (m, 1 H, Py *p*-C*H*), 6.07 (d, $^3J_{HH}$ = 7.8 Hz, 1 H, Py *o*-C*H*), 4.21 (m, 1 H, C*H*(CH_3)$_2$), 3.87 (m, 2 H, N-CH_2-), 3.76 (m, 1 H, C*H*(CH_3)$_2$), 3.62 (m, 2 H, N-CH_2-), 3.47 (m, 1 H, C*H*(CH_3)$_2$), 3.05 (m, 1 H, C*H*(CH_3)$_2$), 2.75 (m, 2 H, Py-CH_2-), 2.54 (m, 2 H, Py-CH_2-), 1.49 (s, 9 H, C(CH_3)$_3$), 1.25 (s, 9 H, C(CH_3)$_3$), 0.04–1.65 ppm (m, 42 H, C(CH_3)$_3$, CH(CH_3)$_2$); ^{13}C NMR (100.61 MHz, C_6D_6, 297.3 K): δ 176.7 (^{q}C), 165.0 (Py *i*-C), 164.5 (^{q}C), 162.8 (Py *i*-C), 151.8 (Dipp *i*-C), 149.9 (Py N-CH), 146.9 (Dipp *i*-C), 146.7 (Py N-CH), 142.2/142.0 (Dipp *o*-C), 138.4/138.2 (Py, *m*-C), 125.4/124.7 (Py, *o*-C), 123.6 (Dipp *m*-C), 122.3 (Dipp *p*-C), 121.6 (Py *p*-C), 121.6 (Dipp *m*-C), 121.1 (Py *p*-C), 118.0 (Dipp *p*-C), 49.2/46.7 (N-CH_2-), 40.3 (C(CH_3)$_3$), 40.0/38.1 (Py-CH_2-), 30.2/30.0 (C(CH_3)$_3$), 29.3 (C*H*(CH_3)$_2$), 28.9 (C*H*(CH_3)$_2$), 25.2 (CH(CH_3)$_2$), 24.2/14.0 ppm (CH(CH_3)$_2$); MS (DEI): *m/z* (%) 753 (1, $[M]^+$), 739 (1, $[C_{47}H_{66}MgN_6]^+$), 722 (1, $[C_{46}H_{62}MgN_6]^+$), 710 (2, $[C_{45}H_{61}MgN_6]^+$), 648 (10, $[C_{41}H_{62}MgN_5]^+$), 365 (100, $[L]^+$), 322 (50, $[C_{21}H_{28}N_3]^+$), 308 (17, $[C_{20}H_{26}N_3]^+$), 260 (44, $[C_{17}H_{28}N_2]^+$) 244 (27, $[C_{16}H_{24}N_2]^+$; $[C_{17}H_{27}N]^+$), 203 (68, $[C_{13}H_{19}N_2]^+$), 106 (43, $[C_7H_8N]^+$), 93 (30, $[C_6H_7N]^+$), 57 (21, $[C_3H_7N]^+$), 41 (30, $[C_2H_3N]^+$); IR (pure): $\tilde{\nu}$ = 2957 (w), 2927 (w), 2866 (w), 1650 (w), 1588 (w), 1530 (w), 1462 (w), 1432 (w), 1380 (w), 1359 (w), 1329 (w), 1259 (w), 1230 (w), 1095 (w), 1011 (w), 935 (w), 786 (w), 769 (w), 747 (w), 674 cm^{-1} (w). Due to the sensitivity of this compound during handling and weighing, no reliable CHN elemental analysis data were obtained.

Synthesis of [(thf)$_2$Na{Dipp-N=C(*t*Bu)-N(H)}] (4 a): A solution of **1** (291 mg, 0.8 mmol) in THF (4 mL) was added to a solution of NaN($SiMe_3$)$_2$ (160 mg, 0.9 mmol) in THF (5 mL) at RT and the reaction mixture was stirred at RT for 24 h. Thereafter, all volatiles were removed in vacuo and 107 mg of **4 a** (31 %) were isolated as yellow crystals after recrystallization from THF and dried in vacuo (which removes ligated ether). M.p. 145–147 °C (dec.); ^{1}H NMR (300.19 MHz, C_6D_6, 299.1 K): δ 7.14 (m, 1 H, Dipp *p*-C*H*), 7.07 (m, 2 H, Dipp *m*-C*H*), 3.49–3.42 (broad, 2 H, N*H*), 3.42 (broad, 2 H, N*H*), 3.04 (sept, $^3J_{HH}$ = 6.6 Hz, 2 H, C*H*(CH_3)$_2$), 1.19 (m, 12 H, CH(CH_3)$_2$), 1.06 ppm (s, 9 H, C(CH_3)$_3$); ^{13}C NMR (100.61 MHz, C_6D_6, 297.0 K): δ 161.1 (^{q}C), 145.5 (Dipp *i*-C), 138.9 (Dipp *o*-C), 123.6 (Dipp *m*-C), 123.2 (Dipp *p*-C), 37.0 (*C*(CH_3)$_3$), 28.5 (C(CH_3)$_3$, *C*H(CH_3)$_2$), 23.7 (CH(CH_3)$_2$), 23.6 ppm (CH(CH_3)$_2$); MS (DEI): *m/z* (%) 427 (5, $[M]^+$), 413 (5, $[M - CH_3]^+$), 260 (20, $[C_{17}H_{28}N_2]^+$), 244 (20, $[C_{16}H_{24}N_2]^+$; $[C_{17}H_{27}N]^+$), 229 (10, $[C_{15}H_{21}N_2]^+$; $[C_{16}H_{23}N]^+$), 217 (30, $[C_{14}H_{21}N_2]^+$), 203 (100, $[C_{13}H_{19}N_2]^+$), 186 (30, $[C_{13}H_{16}N]^+$; $[C_{13}H_{16}N]^+$), 146 (20, $[C_{11}H_{14}]^+$; $[C_{10}H_{12}N]^+$), 118 (20, $[C_9H_{10}]^+$), 106 (65, $[C_7H_8N]^+$), 93 (35, $[C_6H_7N]^+$), 77 (20, $[C_5H_3N]^+$), 57 (90, $[C_3H_7N]^+$), 41 (65, $[C_2H_3N]^+$); MS (Micro-ESI pos. in THF+MeOH): *m/z* (%) 261 (100, $[C_{17}H_{29}N_2]^+$), 244 (30, $[C_{16}H_{24}N_2]^+$; $[C_{17}H_{27}N]^+$); IR (pure): $\tilde{\nu}$ = 3497 (vw), 3394 (vw), 2956 (w), 2867 (w), 1647 (w), 1624 (w), 1588 (w), 1523 (w), 1459 (w), 1433 (w), 1395 (w), 1360 (w), 1325 (w), 1252 (m), 1212 (w), 1056 (w), 997 (m), 853 (w), 794 (m), 768 (m), 704 (w), 659 (m), 542 cm^{-1} (w). Due to the sensitivity of this compound during handling and weighing, no reliable CHN elemental analysis data were obtained.

Synthesis of [(thf)$_2$K{Dipp-N=C(tBu)-N(H)}] (4 b): *METHOD 1*: A solution of **1** (295 mg, 0.8 mmol) in THF (5 mL) was added to a suspension of KH (53 mg, 1.3 mmol) in THF (10 mL) at RT, and the reaction mixture was stirred at RT for 24 h. Thereafter, the mixture was filtered and all volatiles were removed in vacuo. 110 mg of **4 b** (31 %) were isolated pale as yellow crystals after recrystallization from THF and dried in vacuo (which removes ligated ether). *METHOD 2*: A solution of **1** (366 mg, 1.0 mmol) in toluene (7.5 mL) was added to a solution of KN($SiMe_3$)$_2$ (199 mg, 1.0 mmol) in toluene (7.5 mL) at RT and the reaction mixture was stirred at RT for 72 h. During this time, formation of a pale orange solid was observed. This precipitate was collected by filtration, consisting of the solvent-free potassium salt (176 mg, 0.59 mmol, 59 %). Recrystallization of the solid from 0.3 mL THF and storage at 5 °C gave **4 b** as pale yellow crystals. M.p. 122–127 °C (dec.); ^{1}H NMR (400.13 MHz, C_6D_6, 297.1 K): δ 7.14 (m, 1 H, Dipp *p*-C*H*), 7.06 (m, 2 H, Dipp *m*-C*H*), 3.42 (broad, 1 H, N*H*), 3.05 (sept, $^3J_{HH}$ = 6.8 Hz, 2 H, C*H*(CH_3)$_2$), 1.20–1.18 (m, 12 H, CH(CH_3)$_2$), 1.06 ppm (s, 9 H, C(CH_3)$_3$). ^{13}C NMR (100.61 MHz, C_6D_6, 297.1 K): δ 161.1 (^{q}C), 145.5 (Dipp *i*-C), 138.9 (Dipp *o*-C), 123.6 (Dipp *m*-C), 123.2 (Dipp *p*-C), 37.0 (*C*(CH_3)$_3$), 28.5 (C(CH_3)$_3$, *C*H(CH_3)$_2$), 23.7/23.6 ppm (CH(CH_3)$_2$); ^{1}H NMR (250.13 MHz, [D_8]THF, 300.0 K): δ 7.02 (m, 2 H, Dipp *m*-C*H*), 6.85 (m, 1 H, Dipp *p*-C*H*), 4.88 (broad, 1 H, N*H*), 2.98 (sept, $^3J_{HH}$ = 6.9 Hz, 2 H, C*H*(CH_3)$_2$), 1.31 (s, 9 H, C(CH_3)$_3$), 1.14 ppm (m, 12 H, CH(CH_3)$_2$); ^{13}C NMR (62.90 MHz, [D_8]THF, 300.0 K): 162.6 (^{q}C), 146.7 (Dipp *i*-C), 139.3 (Dipp *o*-C), 123.5 (Dipp *m*-C), 122.7 (Dipp *p*-C), 37.8 (*C*(CH_3)$_3$), 28.9 (C(CH_3)$_3$), 28.8 *C*H(CH_3)$_2$), 23.8/23.7 ppm (CH(CH_3)$_2$); MS (DEI): *m/z* (%) 260 (52, $[C_{17}H_{28}N_2]^+$), 245 (31, $[C_{16}H_{24}N_2]^+$; $[C_{17}H_{28}N]^+$), 217 (36, $[C_{14}H_{21}N_2]^+$), 203 (27, $[C_{13}H_{19}N_2]^+$), 186 (20, $[C_{13}H_{16}N]^+$; $[C_{13}H_{16}N]^+$), 41 (35, $[C_2H_3N]^+$, 39 (100). IR (pure): $\tilde{\nu}$ = 3499 (vw), 3394 (vw), 2957 (w), 2867 (w) 1647 (w), 1624 (w), 1588 (w), 1473 (w), 1458 (w), 1379 (w), 1325 (w), 1250 (w), 1012 (m), 980 (m), 943 (m), 847 (m), 769 (m), 684 (m), 645 cm^{-1} (m). Due to the sensitivity of this compound during handling and weighing, no reliable CHN elemental analysis data were obtained.

Synthesis of Dipp-N=C(*t*Bu)-NH_2 (5): In order to obtain the hydrolysis product, 8 mL of the reaction mixture of **2 a** including amidine **1** (200 mg, 0.5 mmol) and NaN($SiMe_3$)$_2$ (100 mg, 0.5 mmol) in THF was treated with water (4 mL) and extracted with toluene (4 mL). The organic layer was collected and after removal of the solvent, the precipitate was recrystallized from *n*-pentane yielding 100 mg of **5** (77 %). M.p. 140–143 °C; ^{1}H NMR (400.13 MHz, $CDCl_3$, 297.0 K): δ 7.10 (m, 2 H, Dipp *m*-C*H*), 6.98 (m, 1 H, Dipp *p*-C*H*), 4.21 (broad, 2 H, NH_2), 2.96 (sept, $^3J_{HH}$ = 6.8 Hz, 2 H, C*H*(CH_3)$_2$), 2.67 (m, 2 H, Py-CH_2-), 1.35 (s, 9 H, C(CH_3)$_3$), 1.16 ppm (m, 12 H, CH(CH_3)$_2$); ^{13}C NMR (100.62 MHz, $CDCl_3$, 298.0 K): δ 162.2 (^{q}C), 144.5 (Dipp *i*-C), 139.2 (Dipp *o*-C), 123.3 (Dipp *m*-C), 122.9 (Dipp *p*-C), 37.1 (*C*(CH_3)$_3$), 28.7 (C(CH_3)$_3$), 28.0 (CH(CH_3)$_2$), 23.8/23.4 ppm (CH(CH_3)$_2$); MS (DEI): *m/z* (%) 308 (1, $[M+EtOH]^+$), 260 (80, $[M]^+$), 245 (50, $[C_{17}H_{27}N]^+$; $[C_{16}H_{25}N_2]^+$), 229 (10, $[C_{16}H_{23}N]^+$; $[C_{15}H_{21}N_2]^+$), 217 (70, $[C_{14}H_{21}N_2]^+$), 203 (100, $[C_{13}H_{19}N_2]^+$), 186 (40, $[C_{12}H_{14}N_2]^+$; $[C_{13}H_{16}N]^+$), 175 (15, $[C_{11}H_{15}N_2]^+$), 160 (10, $[C_{10}H_{12}N_2]^+$), 144 (15, $[C_{10}H_{10}N]^+$), 130 (10, $[C_9H_8N]^+$), 115 (10, $[C_8H_5N]^+$), 91 (10, $[C_7H_7]^+$), 77 (5, $[C_6H_5]^+$), 57 (15, $[C_4H_9]^+$; $[C_3H_7N]^+$), 43 (5, $[C_3H_7]^+$), 41 (15, $[CHN_2]^+$), 29 (5, $[C_2H_5]^+$); IR (pure): $\tilde{\nu}$ = 3498 (w), 3395 (w), 3057 (vw), 2958 (m), 2866 (m), 1646 (s), 1624 (m), 1587 (s), 1521 (m), 1473 (m), 1460 (m), 1433 (m), 1394 (m), 1378 (m), 1360 (m), 1346 (m), 1325 (m), 1254 (m), 1212 (m), 1177 (w), 1148 (w), 1102 (m), 1056 (m), 1038 (m), 935 (m), 866 (m), 832 (m), 797 (m), 768 (s), 747 (m), 724 (m), 684 cm^{-1} (w); elemental analysis (%) calcd for $C_{17}H_{28}N$ (260.42 g mol^{-1}): C, 78.41; H 10.84; N 10.76; found: C, 77.33; H, 10.28; N, 10.39.

Synthesis of [(tmeda)Li{Dipp-N=C(*t*Bu)-N-C_2H_4-Py}] (6): To a suspension of [$(Et_2O)LiN(SiMe_3)_2$] (160 mg, 0.66 mmol) in a mixture of TMEDA (0.6 mL) and toluene (3 mL) was added a solution of **1** (215 mg, 0.6 mmol) in toluene (5 mL) at RT. The reaction mixture was stirred at RT for 24 h and thereafter, concentrated to a volume of approximately 2 mL. Storage at −20 °C for several days led to formation of pale yellow crystals of **6**, which were collected by filtration and washed with *n*-pentane (113 mg, 23 %). Physical data of the residue show that a mixture of **6** and **1** in a ratio of 5:1 was present. M.p. 111–113 °C (dec.); ^{1}H NMR (400.13 MHz, C_6D_6, 297.0 K): δ 7.79 (broad, 1 H, Py N-C*H*), 7.30 (m, 2 H, Dipp *m*-C*H*), 7.08 (m, 1 H, Dipp *p*-C*H*), 7.01 (m, 1 H, Py *m*-C*H*), 6.61 (m, 1 H, Py *o*-C*H*), 6.51 (m, 1 H, Py *p*-C*H*), 3.65 (m, 2 H, C*H*$(CH_3)_2$), 3.28 (m, 2 H, N-CH_2-), 2.36 (broad, 2 H, Py-CH_2-), 2.00–1.98 (m, 16 H, tmeda N-CH_2-, tmeda N(CH_3)$_2$), 1.49 (broad, 2 H, C(CH_3)$_3$), 1.49–1.45 (m, 17 H, C(CH_3)$_3$, CH(CH_3)$_2$), 0.97 ppm (broad, 2 H, CH(CH_3)$_2$); ^{13}C NMR (100.61 MHz, C_6D_6, 297.0 K): δ 163.1 (^{q}C), 153.6 (Dipp *i*-C), 146.6 (Py N-C*H*), 137.6 (Dipp *o*-C), 137.0 (Py *m*-C), 123.7 (Py *o*-C), 121.3 (Dipp *m*-C), 120.7 (Py *p*-C), 116.6 (Dipp *p*-C), 57.6 (tmeda, N-CH_2-), 49.5 (N-CH_2-), 46.1 (tmeda, N(CH_3)$_2$), 40.3 (Py-CH_2-), 39.9 (Py-CH_2-), 31.5 (C(CH_3)$_3$), 28.6 (CH(CH$_3$)$_2$), 24.3/22.6 ppm (CH(CH_3)$_2$); ^{7}Li{^{1}H} NMR (155.51 MHz, C_6D_6, 297.0 K): δ 1.11 (broad, major), −1.47 ppm (broad, minor); MS (DEI): *m/z* (%) 379 (2, $[Li_2L]^+$), 366 (25, $[L+H]^+$), 365 (95, $[L]^+$), 322 (85, $[C_{21}H_{28}N_3]^+$), 308 (35, $[C_{20}H_{26}N_3]^+$), 260 (20, $[C_{17}H_{28}N_2]^+$) 244 (30, $[C_{16}H_{23}N_2]^+$; $[C_{17}H_{27}N]^+$), 229 (100, $[C_{16}H_{23}N]^+$; $[C_{15}H_{21}N_2]^+$), 203 (50, $[C_{13}H_{19}N_2]^+$), 186 (40, $[C_{12}H_{14}N_2]^+$; $[C_{13}H_{16}N]^+$), 172 (10, $[C_{11}H_{12}N_2]^+$; $[C_{12}H_{14}N]^+$), 146 (20, $[C_{11}H_{14}]^+$; $[C_{10}H_{12}N]^+$), 116 (10, $[C_9H_8]^+$; $[C_8H_6N]^+$), 106 (75, $[C_7H_8N]^+$), 91 (10, $[C_7H_7]^+$), 58 (50, $[C_3H_8N]^+$), 41 (8, $[C_2H_3N]^+$); IR (pure): $\tilde{\nu}$ = 3325 (b), 2952 (m), 2863 (m), 2831 (m), 2792 (m), 1656 (m), 1587 (m), 1567 (w), 1532 (s), 1465 (m), 1438 (s), 1420 (m), 1381 (m), 1362 (m), 1343 (m), 1312 (m), 1288 (m), 1260 (m), 1229 (m), 1211 (m), 1173 (m), 1152 (m), 1096 (w), 1045 (m), 1032 (m), 1017 (m), 944 (m), 935 (m), 913 (m), 823 (w), 781 (m), 768 (m), 744 (s), 726 (m), 680 (w), 635 cm^{-1} (w). Due to the sensitivity of this compound during handling and weighing, no reliable CHN elemental analysis data were obtained.

Synthesis of [(thf)$_4$Ca{Dipp-N=C(*t*Bu)-N(H)}$_2$] (7): The reaction mixture of **1** (360 mg, 1.0 mmol) and KN$(SiMe_3)_2$ (390 mg, 2.0 mmol) in THF (6 mL) was stirred at RT for 4 h. Thereafter, the mixture was added to a suspension of CaI_2 (550 mg, 2.2 mmol) in THF (15 mL) and stirred for a further 72 h at RT. All volatiles were removed in vacuo. The remainder was suspended in toluene (18 mL), filtered and the resulting filtrate was concentrated. Adding THF (4 mL) and storage for several days at −20 °C led to the formation of 240 mg of **7** (29 % yield) as colorless crystals. Drying in vacuo caused partial loss of ligated ether. M.p. 112 °C (dec.); ^{1}H NMR (400.20 MHz, C_6D_6, 300.0 K): δ 7.23 (m, 4 H, Dipp *m*-C*H*), 7.12 (m, 2 H, Dipp *p*-C*H*), 3.58 (broad, 6 H, thf O-CH_2-) 3.52 (broad, 2 H, N*H*), 3.13 (sept, $^3J_{HH}$ = 6.8 Hz, 4 H, C*H*$(CH_3)_2$), 1.42 (broad, 6 H, thf, -CH_2-), 1.27 (m, 24 H, CH(CH_3)$_2$), 1.15 ppm (s, 18 H, C(CH_3)$_3$); ^{13}C NMR (100.63 MHz, C_6D_6, 300.0 K): δ 161.2 (^{q}C), 145.6 (Dipp *i*-C), 138.9 (Dipp *o*-C), 123.6 (Dipp *m*-C), 123.2 (Dipp *p*-C), 67.9 (thf, O-CH_2-), 37.0 (C(CH$_3$)$_3$), 28.5 (C(CH_3)$_3$, CH(CH$_3$)$_2$), 25.8 (thf, -CH_2-), 23.7 (CH(CH_3)$_2$), 23.6 ppm (CH(CH_3)$_2$); MS (DEI): *m/z* (%) 260 (100, $[C_{17}H_{28}N_2]^+$), 245 (83, $[C_{16}H_{24}N_2]^+$; $[C_{17}H_{28}N]^+$), 217 (93, $[C_{14}H_{21}N_2]^+$), 203 (35, $[C_{13}H_{19}N_2]^+$), 186 (65, $[C_{13}H_{16}N]^+$; $[C_{13}H_{16}N]^+$), 146 (15, $[C_{11}H_{14}]^+$; $[C_{10}H_{12}N]^+$), 106 (20, $[C_7H_8N]^+$), 91 (20, $[C_6H_5N]^+$), 77 (10, $[C_5H_3N]^+$), 57 (30, $[C_3H_7N]^+$), 41 (20, $[C_2H_3N]^+$); IR (pure): $\tilde{\nu}$ = 3499 (vw), 3395 (w), 2960 (w), 2868 (w), 1647 (w), 1624 (w), 1587 (m), 1529 (w), 1477 (w), 1461 (w), 1434 (w), 1394 (w), 1378 (w), 1359 (w), 1347 (w), 1326 (w), 1254 (w), 1212 (w), 1178 (w), 1157 (w), 1104 (w), 1057 (w), 1036 (w), 936 (m), 867 (w), 833 (w), 798 (w), 769 (m), 742 (w), 725 cm^{-1} (w). Due to the sensitivity of this compound during handling and weighing, no reliable CHN elemental analysis data were obtained.

Synthesis of N-(2,6-diisopropylphenyl)-*N*′-(2-pyridyl)ethyl formamidine (Dipp-N=C(H)-N(H)-C_2H_4-Py) (8): Dipp-NH_2 (10.6 mL, 56.4 mmol), triethylorthoformate (11.2 mL, 56.4 mmol), and 10 μL of a 12 M aqueous HCl (0.02 equiv) were mixed and stirred at 140 °C for 4 h. After distillation (0.085 mbar, 105 °C), 12.81 g of Dipp-N(H) = C(H)OEt (54.9 mmol, 97 %) were isolated. The purity of the product was monitored by use of NMR spectroscopy. The reaction mixture of Dipp-N(H) = C(H)OEt (3.17 g, 13.6 mmol), $NH_2C_2H_4$-Py (1.61 mL, 13.6 mmol), and 10 μL of a 12 M aqueous HCl (0.01 equiv) was stirred at 120 °C for 24 h. The crude product was precipitated with *n*-pentane and recrystallized from a mixture of ethyl acetate and petroleum ether (3:7) yielding 1.23 g of **8** (29 %). The same procedure as a one-pot-synthesis using Dipp-NH_2 (4.2 mL, 22.6 mmol), triethyl orthoformate (3.7 mL, 22.6 mmol), 0.1 mL glacial acetic acid, and $NH_2C_2H_4$-Py (2.68 mL, 22.6 mmol) also led to the formation of **8** (2.48 g, 36 %). Physical data show a coexistence of two isomeric structures of **8** in solution at RT in a ratio of 4:1. M.p. 75 °C. In the ^{1}H NMR spectra the intensity has been adjusted so that both isomers together give integers; the ratio of the major to the minor component is 4:1; ^{1}H NMR (400.13 MHz, $CDCl_3$, 298.0 K): δ 8.55 (m, 0.8 H, Py N-C*H* major), 8.43 (m, 0.2 H, Py N-C*H* minor), 7.63 (td, $^3J_{HH}$ = 7.7 Hz, $^4J_{HH}$ = 1.7 Hz, 0.8 H, Py *m*-C*H* major), 7.56 (m, 0.2 H, Py *m*-C*H* minor), 7.22–7.20 (m, 2 H, Dipp *p*-CH, NC(*H*)N), 7.16 (m, 1 H, Py *p*-C*H*), 7.08 (m, 2 H, Dipp *m*-C*H*), 7.00 (m, 1 H, Py *o*-CH), 5.21 (broad, 1 H, N*H*), 4.63 (broad, 1 H, N*H*), 3.85 (m, 1.6 H, N-CH_2- major) 3.55 (m, 0.4 H, N-CH_2- minor), 3.14–3.08 (m, 3.2 H, C*H*$(CH_3)_2$ major, Py-CH_2- major), 2.98–2.87 (m, 0.8 H, C*H*$(CH_3)_2$ minor, Py-CH_2- minor), 1.15 (d, $^3J_{HH}$ = 6.8 Hz, 9 H, CH(CH_3)$_2$ major), 1.10 ppm (m, 3 H, CH(CH_3)$_2$ minor); ^{13}C NMR (100.61 MHz, $CDCl_3$, 298.0 K): δ 159.8/158.3 (Py *i*-C), 149.5/149.5 (Py N-CH), 148.8 (NC(H)N), 147.7/143.5 (Dipp *i*-C), 140.5/139.3 (Dipp *o*-C), 136.7/136.5 (Py, *m*-C), 123.7/123.6 (Py, *o*-C), 123.4/123.3 (Dipp *p*-C), 122.8 (Dipp *m*-C), 121.7/121.7 (Py *p*-C), 43.9/39.7 (N-CH_2-), 40.8/37.7 (Py-CH_2-), 27.9/27.9 (CH(CH$_3$)$_2$), 23.8/23.6 ppm (CH(CH_3)$_2$); MS (DEI): *m/z* (%) 309 (40, $[M]^+$), 266 (10, $[C_{17}H_{20}N_3]^+$), 203 (10, $[C_{13}H_{19}N_2]^+$), 186 (15, $[C_{12}H_{14}N_2]^+$; $[C_{13}H_{16}N]^+$), 172 (15, $[C_{11}H_{10}N_2]^+$; $[C_{13}H_{16}]^+$), 158 (15, $[C_{10}H_{10}N_2]^+$; $[C_{11}H_{12}N]^+$), 146 (25, $[C_{11}H_{14}]^+$; $[C_{10}H_{12}N]^+$), 130 (20, $[C_{10}H_{10}]^+$; $[C_9H_8N]^+$), 106 (80, $[C_7H_8N]^+$), 93 (100, $[C_6H_7N]^+$), 78 (20, $[C_5H_4N]^+$), 65 (15, $[C_5H_5]^+$), 43 (20, $[C_3H_7]^+$); IR (pure): $\tilde{\nu}$ = 3025 (b), 3050 (w), 2960 (w), 2929 (w), 2867 (w), 1659 (s), 1628 (m), 1584 (m), 1566 (m), 1460 (m), 1430 (m), 1394 (w), 1380 (w), 1361 (w), 1316 (w), 1257 (m), 1186 (w), 1157 (m), 1107 (w), 1096 (w), 1076 (w), 1051 (w), 986 (m), 845 (w), 795 (w), 783 (m), 770 (s), 748 (m), 701 (w), 604 cm^{-1} (w); elemental analysis (%) calcd for $C_{20}H_{27}N_3$ (309.45 g mol^{-1}): C, 77.63; H 8.79; N 13.58; found: C, 77.63; H, 8.79; N, 13.78.

Synthesis of [(thf)Na{Dipp-N=C(H)-N-C_2H_4-Py}]$_2$ (9a); A solution of **8** (340 mg, 1.1 mmol) in toluene (7 mL) was added to a solution of NaN$(SiMe_3)_2$ (260 mg, 1.4 mmol) in toluene (7 mL) at RT, and the reaction mixture was stirred at RT for 24 h. Thereafter, the reaction mixture was concentrated to a volume of about 2 mL and restocked with THF (10 mL). The mixture was stirred at 60 °C for 30 min and the resulting solution was concentrated to a volume of approximately 1 mL. Addition of toluene (2 mL) and storage at 5 °C for several days led to the formation of 170 mg of **9a** (38 %). M.p. 169 °C (dec.); ^{1}H NMR (400.13 MHz, C_6D_6, 297.0 K): δ 8.22 (broad, 1 H, Py N-C*H*), 7.63 (broad, 1 H, NC(*H*)N) 7.18 (m, 2 H, Dipp *m*-C*H*), 7.08–7.02 (m, 2 H, Py *m*-C*H*, Dipp *p*-C*H*), 6.70 (m, 1 H, Py *o*-C*H*), 6.57 (m, 1 H, Py *p*-C*H*), 3.64–3.50 (m, 8 H, N-CH_2-, thf O-CH_2-, C*H*$(CH_3)_2$), 2.90 (m, 2 H, Py-CH_2-), 1.45 (m, 4 H, thf, -CH_2-), 1.20 ppm (d, $^3J_{HH}$ = 6.8 Hz, 12 H, CH(CH_3)$_2$); ^{13}C NMR (100.61 MHz, C_6D_6,

297.0 K): δ 170.0 (NC(H)N), 163.1 (Py *i*-*C*), 151.4 (Dipp *i*-*C*), 148.8 (Py N-*C*H), 142.4 (Dipp *o*-*C*), 137.1 (Py, *m*-*C*), 124.1 (Py, *o*-*C*), 123.2 (Dipp *m*-*C*), 121.4 (Dipp *p*-*C*), 121.2 (Py *p*-*C*), 67.9 (thf O-*C*H_2-), 55.9 (N-*C*H_2-), 42.4 (Py-*C*H_2-), 28.1 (*C*H(CH_3)$_2$), 25.8 (thf -*C*H_2-), 24.6 ppm (CH(*C*H_3)$_2$); MS (DEI): *m/z* (%) 309 (100, $[L]^+$), 266 (25, $[C_{17}H_{20}N_3]^+$), 203 (25, $[C_{13}H_{19}N_2]^+$), 186 (20, $[C_{12}H_{14}N_2]^+$; $[C_{13}H_{16}N]^+$), 172 (30, $[C_{11}H_{10}N_2]^+$; $[C_{13}H_{16}]^+$), 159 (15, $[C_{10}H_{11}N_2]^+$; $[C_{11}H_{13}N]^+$), 146 (20, $[C_{11}H_{14}]^+$; $[C_{10}H_{12}N]^+$), 106 (20, $[C_7H_8N]^+$), 93 (15, $[C_6H_7N]^+$), 29 (15, $[C_2H_5]^+$); (Micro-ESI pos. in THF+MeOH): *m/z* (%) 310 (100, $[L+H]^+$), 291 (8, $[C_{19}H_{21}N_3]^+$), 205 (85, $[C_{13}H_{21}N_2]^+$), 106 (10, $[C_7H_8N]^+$). IR (pure): $\tilde{\nu}$ = 3205 (vw), 3050 (vw), 3014 (w), 2957 (w), 2934 (w), 2867 (w), 2804 (vw), 1661 (w), 1642 (w), 1629 (w), 1594 (w), 1585 (w), 1564 (w), 1552 (m), 1461 (w), 1431 (m), 1380 (w), 1343 (w), 1331 (w), 1256 (w), 1214 (w), 1187 (w), 1159 (w), 1108 (w), 1097 (w), 1055 (w), 1000 (m), 986 (w), 845 (w), 796 (w), 782 (w), 772 (w), 760 (m), 701 (w), 608 cm^{-1} (w). Due to the sensitivity of this compound during handling and weighing no reliable, CHN elemental analysis data were obtained.

Synthesis of [(thf)K{Dipp-N=C(H)-N-C_2H_4-Py}]$_2$ (9b): A solution of **8** (320 mg, 1.0 mmol) in toluene (7.5 mL) was added to a solution of KN($SiMe_3$)$_2$ (250 mg, 1.2 mmol) in toluene (7.5 mL) at RT, and the reaction mixture was stirred at RT for 24 h. The resulting precipitate was collected by filtration and recrystallized from THF (2 mL) yielding 200 mg of **9b** after storage at −20 °C for several hours (47% yield). Drying in vacuo partly removes ligated ether. M.p. 157 °C (dec.); ^{1}H NMR (400.13 MHz, [D_8]THF, 297.1 K): δ 8.43 (broad, 1H, Py N-C*H*), 7.55–6.60 (m, 7H, NC(*H*)N, H_{Aryl}), 3.81/3.53 (m, 2H, N-CH_2-), 3.23–2.89 (m, 4H, Py-CH_2-, C*H*(CH_3)$_2$), 1.11–1.06 ppm (m, 12H, CH(CH_3)$_2$); ^{13}C NMR (100.61 MHz, [D_8]THF, 297.0 K): δ 166.5 (NC(H)N), 164.1 (Py *i*-*C*), 150.3 (Dipp *i*-*C*), 149.5 (Py N-*C*H), 141.9 (Dipp *o*-*C*), 136.9 (*C*H_{Aryl}), 124.3 (*C*H_{Aryl}), 122.9 (*C*H_{Aryl}), 121.6 (*C*H_{Aryl}), 119.4 (*C*H_{Aryl}), 58.1 (N-*C*H_2-), 44.3 (Py-*C*H_2-), 28.7 (*C*H(CH_3)$_2$), 24.3 ppm (CH(*C*H_3)$_2$); MS (DEI): *m/z* (%) 309 (100, $[L]^+$), 266 (35, $[C_{17}H_{20}N_3]^+$); MS (DEI): *m/z* (%) 839 (2, $[M_2]^+$), 765 (1, [M_2 - THF]$^+$), 355 (20), 341 (15), 309 (100, $[L]^+$), 281 (60, $C_{18}H_{23}N_3]^+$), 266 (35, $[C_{17}H_{20}N_3]^+$), 230 (30, $[C_{15}H_{22}N_2]^+$; $[C_{16}H_{24}N]^+$), 203 (83, $[C_{13}H_{19}N_2]^+$), 172 (90, $[C_{11}H_{10}N_2]^+$; $[C_{13}H_{16}]^+$), 146 (80, $[C_{11}H_{14}]^+$; $[C_{10}H_{12}N]^+$), 106 (90, $[C_7H_8N]^+$), 93 (75, $[C_6H_7N]^+$), 43 (10, $[C_3H_7]^+$); IR (pure): $\tilde{\nu}$ = 3499 (vw), 3054 (vw), 2958 (w), 2865 (w), 2810 (vw), 1658 (m), 1643 (m), 1631 (m), 1585 (m), 1566 (w), 1549 (m), 1460 (m), 1431 (w), 1381 (w), 1359 (w), 1331 (w), 1255 (w), 1203 (w), 1161 (w), 1109 (w), 1076 (w), 1054 (m), 986 (w), 844 (w), 796 (w), 782 (m), 761 (m), 746 (w), 630 (w), 606 cm^{-1} (w). Due to the sensitivity of this compound during handling and weighing, no reliable CHN elemental analysis data were obtained.

Crystal structure determinations: The intensity data for the compounds were collected on a Nonius KappaCCD diffractometer using graphite-monochromated $Mo_{K\alpha}$ radiation. Data was corrected for Lorentz and polarization effects; absorption was taken into account on a semi-empirical basis using multiple-scans.[27–29] The structures were solved by direct methods (SHELXS)[29] and refined by full-matrix least squares techniques against F_o^2 (SHELXL-97).[30] All hydrogen atoms bound to the compounds **1**, **3**, **4b**, **7** (both with exception of the disordered thf-molecules), and **9a** as well as the hydrogen atoms of the amine groups of **4a** and **5** and those of the methylene groups C3A and C19B of **6** were located by difference Fourier synthesis and refined isotropically. All other hydrogen atoms were included at calculated positions with fixed thermal parameters. All non-disordered and non-hydrogen atoms were refined anisotropically.[30] The crystal of **9b** contains large voids, filled with disordered solvent molecules. The size of the voids are 215 Å^3 per unit cell. Their contribution to the structure factors was secured by back-Fourier transformation using the SQUEEZE routine of the program PLATON[31] resulting in 56 electrons/unit cell. The

Table 4. Crystal data and refinement details for the X-ray structure determinations of the compounds **1**–**4**.

Compound	**1**	**2a**	**2b**	**3**	**4a**	**4b**
formula	$C_{24}H_{35}N_3$	$C_{30}H_{52}CaN_4Si_2$	$C_{30}H_{52}N_4Si_2Sr$	$C_{48}H_{68}MgN_6$	$C_{25}H_{43}N_2NaO_2$	$C_{21}H_{32}KN_2O$
M_r [g mol^{-1}]	365.55	565.02	612.56	753.39	426.60	367.59
T [°C]	−140(2)	−140(2)	−140(2)	−140(2)	−140(2)	−140(2)
crystal system	monoclinic	Monoclinic	monoclinic	monoclinic	tetragonal	monoclinic
space group	*P* $2_1/n$	*P* $2_1/n$	*P* $2_1/n$	*P* $2_1/c$	*I* 4_1 *c d*	*C* 2/*c*
a [Å]	14.6120(2)	12.3412(5)	12.4750(3)	12.7330(2)	21.4723(3)	12.6807(4)
b [Å]	19.6459(2)	15.7404(6)	15.8620(4)	20.4882(4)	21.4723(3)	19.3139(5)
c [Å]	16.6619(2)	18.1095(7)	17.9909(4)	18.3784(3)	22.5062(3)	18.4522(6)
α [°]	90	90	90	90.00	90	90
β [°]	110.987(1)	105.762(2)	106.659(2)	107.575(1)	90	100.080(1)
γ [°]	90	90	90	90.00	90	90
V [Å^3]	4465.76(9)	3385.6(2)	3410.59(14)	4570.69(14)	10376.7(2)	4449.4(2)
Z	8	4	4	4	16	8
ρ [g cm^{-3}]	1.087	1.109	1.193	1.095	1.092	1.097
μ [cm^{-1}]	0.64	2.8	16.74	0.77	0.82	2.49
measured data	35159	20736	19616	32520	11137	12606
data with $I > 2\sigma(I)$	8178	5723	5914	8614	5089	4074
unique data (R_{int})	10216/0.0411	7505/0.0853	7750/0.0663	10402/0.0364	5904/0.0293	5074/0.0377
wR_2 (all data, on F^2)[a]	0.1123	0.1437	0.1097	0.1169	0.1055	0.1902
R_1 ($I > 2\sigma(I)$)[a]	0.0477	0.0742	0.0547	0.0492	0.0471	0.0686
s[b]	1.084	1.167	1.131	1.063	1.090	1.096
res. dens. [e·Å^{-3}]	0.236/−0.172	0.347/−0.319	0.521/−0.311	0.284/−0.258	0.177/−0.142	0.829/−0.382
Flack parameter	–	–	–	–	0.2(3)	–
absorpt method	multi-scan	multi-scan	multi-scan	multi-scan	multi-scan	multi-scan
absorpt corr $T_{min}/_{max}$	0.7136/0.7456	0.5326/0.7456	0.5092/0.7456	0.7167/0.7456	0.7099/0.7418	0.6428/0.7456
CCDC	1462997	1462998	1462999	1463000	1463001	1463002

[a] Definition of the R indices: $R_1 = (\Sigma||F_o| - |F_c||)/\Sigma|F_o|$; $wR_2 = \{\Sigma[w(F_o^2 - F_c^2)^2]/\Sigma[w(F_o^2)^2]\}^{1/2}$ with $w^{-1} = \sigma^2(F_o^2) + (aP)^2 + bP$; $P = [2F_c^2 + \mathrm{Max}(F_o^2)]/3$. [b] $s = \{\Sigma[w(F_o^2 - F_c^2)^2]/(N_o - N_p)\}^{1/2}$.

Table 5. Crystal data and refinement details for the X-ray structure determinations of the compounds **5–9**.

Compound	**5**	**6**	**7**	**8**	**9a**	**9b**
formula	$C_{19}H_{34}N_2O$	$C_{30}H_{50}LiN_5$	$C_{50}H_{83}CaN_4O_4$	$C_{20}H_{27}N_3$	$C_{24}H_{34}N_3NaO$	$C_{25}H_{36}KN_3O_{1.25}$[c]
M_r [g mol^{-1}]	306.48	487.69	844.28	309.45	403.53	437.67[c]
T [°C]	−140(2)	−140(2)	−140(2)	−140(2)	−140(2)	−140(2)
crystal system	monoclinic	monoclinic	monoclinic	tetragonal	orthorhombic	triclinic
space group	$P\,2_1/n$	$P\,2_1/c$	$P\,2_1/n$	$P\,4_1$	$P\,b\,c\,a$	$P\,\bar{1}$
a [Å]	11.2274(3)	21.9283(3)	10.0022(2)	9.0286(1)	14.1180(3)	10.1600(2)
b [Å]	16.5606(4)	15.4886(3)	21.2034(4)	9.0286(1)	15.8834(3)	14.6984(2)
c [Å]	11.8370(2)	18.1164(3)	24.2187(3)	44.6099(8)	20.9616(5)	18.3533(3)
α [°]	90	90	90	90	90	85.666(1)
β [°]	115.632(1)	103.499(1)	93.124(1)	90	90	77.389(1)
γ [°]	90	90	90	90	90	84.115(1)
V [Å^3]	1984.30(8)	5983.04(17)	5128.69(15)	3636.40(9)	4700.47(17)	2656.59(8)
Z	4	8	4	8	8	4
ρ [g cm^{-3}]	1.026	1.083	1.093	1.130	1.140	1.094[c]
μ [cm^{-1}]	0.63	0.64	1.66	0.67	0.86	2.2[c]
measured data	11468	33595	37345	25501	32853	18174
data with $I > 2\sigma(I)$	3539	8988	8747	2621	4354	9831
unique data (R_{int})	4530/0.0288	13176/0.0539	11690/0.0575	3634/0.0321	5174/0.0478	11519/0.0221
wR_2 (all data, on F^2)[a]	0.1437	0.1573	0.1592	–	0.1112	0.1336
R_1 ($I > 2\sigma(I)$)[a]	0.0605	0.0763	0.0669	–	0.0485	0.0556
s[b]	1.087	1.114	1.075	–	1.097	1.026
res. dens. [e·Å^{-3}]	0.240/−0.210	0.262/−0.229	0.535/−0.362	0.533/−0.274	0.391/−0.324	0.921/−0.954
absorpt method	multi-scan	multi-scan	multi-scan	multi-scan	multi-scan	multi-scan
absorpt corr $T_{min}/_{max}$	0.6894/0.7456	0.6673/0.7456	0.7014/0.7456	0.7062/0.7456	0.6518/0.7456	0.7027/0.7456
CCDC	1463003	1463004	1463005	motif	1463006	1463007

[a] Definition of the R indices: $R_1 = (\Sigma||F_o|-|F_c||)/\Sigma|F_o|$; $wR_2 = \{\Sigma[w(F_o^2-F_c^2)^2]/\Sigma[w(F_o^2)^2]\}^{1/2}$ with $w^{-1} = \sigma^2(F_o^2)+(aP)^2+bP$; $P = [2F_c^2+\mathrm{Max}(F_o^2)]/3$. [b] $s = \{\Sigma[w(F_o^2-F_c^2)^2]/(N_o-N_p)\}^{1/2}$. [c] Derived parameters do not contain the contribution of the disordered solvent.

crystals of **8** were extremely thin and of low quality, resulting in a substandard data set; however, the structure is sufficient to show connectivity and geometry despite the high final R value. We will only publish the conformation of the molecule and the crystallographic data. We will not deposit the data for **8** at the Cambridge Crystallographic Data Centre. Crystallographic data, structure solution, and refinement details are summarized for all compounds in Tables 4 and 5. XP (SIEMENS Analytical X-ray Instruments, Inc.)[32] was used for structure representations.

NMR and IR spectra as well as the molecular structure of **2b** are provided in the Supporting Information. CCDC 1462997 (**1**), 1462998 (**2a**), 462999 (**2b**), 1463000 (**3**), 1463001 (**4a**), 1463002 (**4b**), 1463003 (**5**), 1463004 (**6**), 1463005 (**7**), 1463006 (**9a**), and 1463007 (**9b**) contain the supplementary crystallographic data for this paper. These data are provided free of charge by The Cambridge Crystallographic Data Centre.

Acknowledgements

We appreciate the financial support by the Fonds der Chemischen Industrie (FCI/VCI, Frankfurt/Main, Germany). C.L. was also supported by a Ph.D. fellowship from the Graduate Academy of the Friedrich Schiller University Jena. Infrastructure was partially provided by the Regional Development Funds of the EU (EFRE).

Keywords: 1,3-diazaallyl anions · alkali metals · alkaline earth metals · formamidinates · pivalamidinates

[1] A. Togni, L. M. Venanzi, *Angew. Chem. Int. Ed. Engl.* **1994**, *33*, 497–526; *Angew. Chem.* **1994**, *106*, 517–547.

[2] a) M. S. Hill, D. J. Liptrot, C. Weetman, *Chem. Soc. Rev.* **2016**, *45*, 972–988; b) Y.-C. Tsai, *Coord. Chem. Rev.* **2012**, *256*, 722–758; c) S. P. Sarish, S. Nembenna, S. Nagendran, H. W. Roesky, *Acc. Chem. Res.* **2011**, *44*, 157–170; d) S. Harder, *Chem. Rev.* **2010**, *110*, 3852–3876; e) A. G. M. Barrett, M. R. Crimmin, M. S. Hill, P. A. Procopiou, *Proc. R. Soc. London, Ser. A* **2010**, *466*, 927–963.

[3] D. Kalden, S. Krieck, H. Görls, M. Westerhausen, *Dalton Trans.* **2015**, *44*, 8089–8099.

[4] a) S. Krieck, A. Koch, K. Hinze, C. Müller, J. Lange, H. Görls, M. Westerhausen, *Eur. J. Inorg. Chem.* **2016**, 2332-2348; b) L. M. D. R. S. Martins, A. J. L. Pombeiro, *Coord. Chem. Rev.* **2014**, *265*, 74–88; c) A. Otero, J. Fernández-Baeza, A. Lara-Sánchez, L. F. Sánchez-Barba, *Coord. Chem. Rev.* **2013**, *257*, 1806–1868; d) H. R. Bigmore, S. C. Lawrence, P. Mountford, C. S. Tredget, *Dalton Trans.* **2005**, 635–651; e) C. Pettinari, R. Pettinari, *Coord. Chem. Rev.* **2005**, *249*, 663–691; f) C. Pettinari, R. Pettinari, *Coord. Chem. Rev.* **2005**, *249*, 525–543; g) A. Otero, J. Fernández-Baeza, A. Antiñolo, J. Tejeda, A. Lara-Sánchez, *Dalton Trans.* **2004**, 1499–1510; h) D. L. Reger, *Comments Inorg. Chem.* **1999**, *21*, 1–28.

[5] a) F. T. Edelmann, *Chem. Soc. Rev.* **2012**, *41*, 7657–7672; b) F. T. Edelmann, *Chem. Soc. Rev.* **2009**, *38*, 2253–2268; c) F. T. Edelmann, *Adv. Organomet. Chem.* **2008**, *57*, 183–352.

[6] S. P. Green, C. Jones, A. Stasch, *Science* **2007**, *318*, 1754–1757; for reviews on subvalent s-block metal complexes, see: a) M. Westerhausen, *Angew. Chem. Int. Ed.* **2008**, *47*, 2185–2187; *Angew. Chem.* **2008**, *120*, 2215–2217; b) S. Krieck, L. Yu, M. Reiher, M. Westerhausen, *Eur. J. Inorg. Chem.* **2010**, 197–216.

[7] S.-O. Hauber, F. Lissner, G. B. Deacon, M. Niemeyer, *Angew. Chem. Int. Ed.* **2005**, *44*, 5871–5875; *Angew. Chem.* **2005**, *117*, 6021–6025.

[8] C. Glock, C. Loh, H. Görls, S. Krieck, M. Westerhausen, *Eur. J. Inorg. Chem.* **2013**, 3261–3269.

[9] C. Loh, S. Seupel, H. Görls, S. Krieck, M. Westerhausen, *Eur. J. Inorg. Chem.* **2014**, 1312–1321.

[10] I. V. Basalov, O. S. Yurova, A. V. Cherkasov, G. K. Fukin, A. A. Trifonov, *Inorg. Chem.* **2016**, *55*, 1236–1244.

[11] a) D. Heitmann, C. Jones, P. C. Junk, K.-A. Lippert, A. Stasch, *Dalton Trans.* **2007**, 187 – 189; b) D. Heitmann, C. Jones, D. P. Mills, A. Stasch, *Dalton Trans.* **2010**, *39*, 1877 – 1882.
[12] C. Loh, S. Seupel, H. Görls, S. Krieck, M. Westerhausen, *Organometallics* **2014**, *33*, 1480 – 1491.
[13] C. Loh, S. Seupel, A. Koch, H. Görls, S. Krieck, M. Westerhausen, *Dalton Trans.* **2014**, *43*, 14440 – 14449.
[14] K. Kincaid, C. P. Gerlach, G. R. Giesbrecht, J. R. Hagadorn, G. D. Whitener, A. Shafir, J. Arnold, *Organometallics* **1999**, *18*, 5360 – 5366.
[15] a) V. H. Gessner, C. Strohmann, *J. Am. Chem. Soc.* **2008**, *130*, 14412 – 14413; b) C. Unkelbach, H. S. Rosenbaum, C. Strohmann, *Chem. Commun.* **2012**, *48*, 10612 – 10614.
[16] A. R. Kennedy, R. E. Mulvey, D. L. Ramsay, S. D. Robertson, *Dalton Trans.* **2015**, *44*, 5875 – 5887. For a review on cleave-and-capture chemistry, see: R. E. Mulvey, *Dalton Trans.* **2013**, *42*, 6676 – 6693.
[17] R. E. Cowley, K. P. Chiang, P. L. Holland, D. Adhikari, F. J. Zuno-Cruz, G. S. Cabrera, D. J. Mindiola in *Inorganic Syntheses, Vol. 35* (Ed.: T. B. Rauchfuss), John Wiley & Sons, Inc., Hoboken, **2010**, pp. 13 – 19.
[18] a) C. Glock, H. Görls, M. Westerhausen, *Inorg. Chem.* **2009**, *48*, 394 – 399; b) C. Glock, H. Görls, M. Westerhausen, *Dalton Trans.* **2011**, *40*, 8108 – 8113; c) C. Glock, H. Görls, M. Westerhausen, *Chem. Commun.* **2012**, *48*, 7094 – 7096; d) C. Glock, S. Ziemann, F. M. Younis, H. Görls, W. Imhof, S. Krieck, M. Westerhausen, *Organometallics* **2013**, *32*, 2649 – 2660.
[19] a) R. P. Davies, *Inorg. Chem. Commun.* **2000**, *3*, 13 – 15; b) A. R. Kennedy, R. E. Mulvey, R. B. Rowlings, *J. Organomet. Chem.* **2002**, *648*, 288 – 292; c) X. He, B. C. Noll, A. Beatty, R. E. Mulvey, K. W. Henderson, *J. Am. Chem. Soc.* **2004**, *126*, 7444 – 7445; d) L. T. Wendell, J. Bender, X. He, B. C. Noll, K. W. Henderson, *Organometallics* **2006**, *25*, 4953 – 4959; e) A. M. Johns, S. C. Chmely, T. P. Hanusa, *Inorg. Chem.* **2009**, *48*, 1380 – 1384; f) M. S. Hill, G. Kociok-Köhn, D. J. MacDougall, *Inorg. Chem.* **2011**, *50*, 5234 – 5241; g) F. Ortu, G. J. Moxey, A. J. Blake, W. Lewis, D. L. Kays, *Inorg. Chem.* **2013**, *52*, 12429 – 12439.
[20] M. Song, B. Donnadieu, M. Soleilhavoup, G. Bertrand, *Chem. Asian J.* **2007**, *2*, 904 – 908.
[21] M. Lindley, P. T. Wolczanski, T. R. Cundari, E. B. Lobkovsky, *Organometallics* **2015**, *34*, 4656 – 4668.
[22] a) P. Jutzi, *J. Organomet. Chem.* **1990**, *400*, 1 – 17; b) T. P. Hanusa, *Chem. Rev.* **1993**, *93*, 1023 – 1036; c) D. J. Burkey, T. P. Hanusa, *Comments Inorg. Chem.* **1995**, *17*, 41 – 77; d) A. J. Bridgeman, *J. Chem. Soc., Dalton Trans.* **1997**, 2887 – 2893; e) S. Harder, *Coord. Chem. Rev.* **1998**, *176*, 17 – 66; f) N. J. Long, *Metallocenes: An Introduction to Sandwich Complexes*, Blackwell Science, Oxford, **1998**; g) P. Jutzi, N. Burford in *Metallocenes: Synthesis Reactivity Applications, Vol. 1* (Eds. A. Togni, R. L. Halterman), Wiley-VCH: Weinheim, **1998**, Chapter 1, pp. 3 – 54; h) P. Jutzi, N. Burford, *Chem. Rev.* **1999**, *99*, 969 – 990; i) P. Jutzi, G. Reumann, *J. Chem. Soc. Dalton Trans.* **2000**, 2237 – 2244; j) T. P. Hanusa, *Organometallics* **2002**, *21*, 2559 – 2571; k) P. H. M. Budzelaar, J. J. Engelberts, J. H. van Lenthe, *Organometallics* **2003**, *22*, 1562 – 1576.
[23] a) M. Westerhausen, W. Schwarz, *Z. Anorg. Allg. Chem.* **1991**, *604*, 127 – 140; b) M. Westerhausen, W. Schwarz, *Z. Anorg. Allg. Chem.* **1991**, *606*, 177 – 190; c) M. Westerhausen, M. Hartmann, N. Makropoulos, B. Wieneke, M. Wieneke, W. Schwarz, D. Stalkec, *Z. Naturforsch., B: J. Chem. Sci.* **1998**, *53*, 117 – 125.
[24] a) M. Westerhausen, *Trends Organomet. Chem.* **1997**, *2*, 89 – 105; b) M. Westerhausen, *Coord. Chem. Rev.* **1998**, *176*, 157 – 210; c) A. Torvisco, A. Y. O'Brien, K. Ruhlandt-Senge, *Coord. Chem. Rev.* **2011**, *255*, 1268 – 1292; d) M. P. Coles, *Coord. Chem. Rev.* **2015**, *297 – 298*, 2 – 23.
[25] K. F. Tesh, T. P. Hanusa, J. C. Huffman, *Inorg. Chem.* **1990**, *29*, 1584 – 1586.
[26] M. Westerhausen, *Inorg. Chem.* **1991**, *30*, 96 – 101.
[27] COLLECT, Data Collection Software; Nonius B. V., Netherlands, **1998**.
[28] Processing of X-Ray Diffraction Data Collected in Oscillation Mode: Z. Otwinowski, W. Minor in: *Methods in Enzymology, Vol. 276, Macromolecular Crystallography, Part A* (Eds. C. W. Carter, R. M. Sweet), Academic Press, **1997**, pp. 307 – 326.
[29] SADABS 2.10, Bruker-AXS Inc., Madison, WI, USA, **2002**.
[30] G. M. Sheldrick, *Acta Crystallogr., Sect. A: Found. Crystallogr.* **2008**, *64*, 112 – 122.
[31] A. L. Spek, *Acta Crystallogr., Sect. D: Biol. Crystallogr.* **2009**, *65*, 148 – 155.
[32] XP, Siemens Analytical X-Ray Instruments Inc., Karlsruhe, Germany, **1990**; Madison, WI, USA, **1994**.

Received: May 3, 2016
Published online on June 29, 2016